Majestic American Journal of Chemistry
Volume 1, **2026**, **pp.** 1-24, **Article ID:** CM2601103006
DOI: 10.65080/majc.v1.CM2601103006

Review Article

Multicomponent Reactions for Bioactive Nitrogen Heterocycles: Key Intermediates, Catalytic Control and Metric-Based Sustainability

Atta Ullah[1, *], ✉, **Chan Yen San**[1]

[1]*Department of Chemical & Energy Engineering, Faculty of Engineering and Science, Curtin University Malaysia, Lot 13149, Block 5, Kuala Baram Land District, CDT 250, 98009 Miri, Sarawak, Malaysia*

Article History

Received: 09 September, 2026 Revised: 07 October, 2026 Accepted: 12 October, 2026 Published: 05 November, 2026

Abstract:

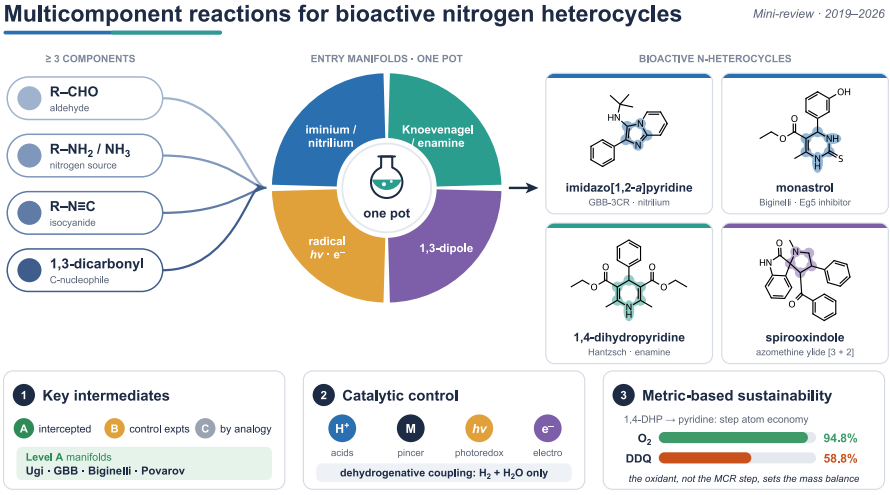
Introduction: Multicomponent Reactions (MCRs) assemble nitrogen heterocycles from three or more components in a single operation and are widely presented as both diversity-generating and inherently sustainable. This mini-review tests both claims against the 2019–2026 literature.

Methodology: Primary studies were identified through database searches and citation tracking and were included when three or more components formed a five- or six-membered nitrogen heterocycle, or a fused or spiro derivative, in one pot. Twenty-four representative methods were then evaluated against the same criteria: the level of mechanistic evidence, catalyst recyclability and the available mass metrics. Rather than cataloguing scaffolds, the review organises MCRs by the electrophile through which the components enter the reaction: iminium and nitrilium ions, Knoevenagel adducts and enaminones, 1,3-dipoles, and photochemically or electrochemically generated radicals. Mechanistic proposals are graded as Level A (intermediate isolated or observed directly, or kinetic evidence), Level B (control experiments only) or Level C (analogy alone).

Results: The Biginelli, Ugi, Groebke–Blackburn–Bienaymé and Povarov manifolds are well characterised, whereas many scaffold-directed cascades are not. Theoretical atom economies, calculated from balanced model equations, show that the terminal oxidation step, not the multicomponent step, sets the mass balance of aromatised products wherever a stoichiometric oxidant is used; the nitrogen source alone changes atom economy by 11–14 percentage points. Experimental metrics such as reaction mass efficiency and process mass intensity are seldom reported, so a common audit protocol is defined for them and kept separate from the calculated values.

Conclusion: The review closes by addressing the gap between reported substrate scope and validated success rates, and by presenting the case for optimisation loops that treat waste and yield as a single objective.

Graphical Abstract



Keywords: Multicomponent reactions, nitrogen heterocycles, reaction mechanisms, green chemistry metrics, heterogeneous catalysis, photoredox catalysis.

*Address correspondence to this author at Department of Chemical & Energy Engineering, Faculty of Engineering and Science, Curtin University Malaysia, Lot 13149, Block 5, Kuala Baram Land District, CDT 250, 98009 Miri, Sarawak, Malaysia; E-mail: atta@postgrad.curtin.edu.my

© 2026 Copyright by the Authors.
Licensed as an open access article using a CC BY 4.0 license.

Cite as: Ullah, A.; San, C.Y. Multicomponent reactions for bioactive nitrogen heterocycles: Key intermediates, catalytic control and metric-based sustainability. *Majes. Amer. J. Chem.*, **2026**, *1*, 1-24. Article ID: CM2601103006. https://doi.org/10.65080/majc.v1.CM2601103006

1. INTRODUCTION

Nitrogen heterocycles form the structural core of modern small-molecule therapeutics. An analysis of United States Food and Drug Administration approvals through 2013 found that 59% of unique small-molecule drugs contained a nitrogen heterocycle [1]. A follow-up study of the 321 new small-molecule drugs approved between 2013 and 2023 put that figure at 82%, and the number of nitrogen heterocycles per drug also rose [2]. Over that period pyridine displaced piperidine as the most frequent ring, pyrimidine, pyrazole and morpholine all climbed the ranking, and fused nitrogen heterocycles became markedly more common, largely because of newly approved oncology agents [2]. The synthetic problem this pose is not whether such rings can be made, but how efficiently libraries of them can be assembled and how much waste the assembly generates.

Multicomponent reactions address the first half of that problem directly. In an MCR, three or more components combine in one vessel so that most or all of their atoms are incorporated into the product, and the intermediates are never isolated [3]. The consequences are practical: fewer unit operations, fewer work-ups and chromatographic separations, and a combinatorial relationship between the number of commercially available inputs and the number of accessible products (Fig. **1A**, **B**). These properties underpin the long-standing argument that MCRs are intrinsically sustainable tools for organic synthesis [4], and they explain the sustained use of isocyanide-based MCRs in medicinal chemistry [5, 6].

The field is well reviewed, but from three directions that leave a gap. Scaffold catalogues organise the literature by ring class; a recent example covers triazoles, imidazoles, pyrazoles, pyrimidines and pyridazines assembled through the Biginelli, Ugi, Hantzsch and Passerini platforms [7]. Platform-specific reviews do the same for the Groebke–Blackburn–Bienaymé (GBB) reaction [8, 9] and for the Povarov and Doebner reactions [10]. Activation-mode reviews cover photochemical and electrochemical MCRs [11] and their combination [12]. Mechanistic reviews grade the evidence behind the classical named reactions [13] and set out how MCR mechanisms should be investigated [14], including the frequently overlooked role of the solvent [15]. What no survey provides is a comparison across these axes: which manifolds are supported by intercepted intermediates rather than analogy, and what the reported methods actually cost in material terms.

This review is organised accordingly. Section 1.1 describes how the literature was selected and evaluated, and Section 1.2 defines the criteria used to grade mechanistic evidence. Section 2 defines terms and classifies platforms by whether the heterocyclic ring is closed within the multicomponent step. Section 3 treats the recurring intermediates and grades the evidence for each manifold. Sections 4 to 8 cover azines, five-membered and fused systems, catalytic strategies, chalcone-derived cascades, and light- and current-driven variants. Section 9 examines sustainability quantitatively and separates calculated from experimentally determined metrics. Atom Economy (AE) is calculated here from balanced model equations, whereas Reaction Mass Efficiency (RME) and Process Mass Intensity (PMI), the metrics that actually track waste [16, 17], require experimental masses and are therefore defined as an audit protocol. Sections 10 and 11 cover medicinal relevance and the unresolved problems.

1.1. Scope and Review Methodology

The review covers primary studies published from January 2019 to the time of writing in 2026. Earlier papers are cited where they are needed to establish a mechanism, a definition or a metric; the Level A assignments for the Ugi and Biginelli manifolds, for example, rest on such earlier studies. The literature was identified by keyword searches of Scopus, Web of Science and Google Scholar, combining "multicomponent reaction" or "one-pot" with named-reaction terms (Biginelli, Hantzsch, Ugi, Groebke–Blackburn–Bienaymé, Povarov, van Leusen, Kröhnke, Bohlmann–Rahtz), ring-class terms (pyridine, pyrimidine, imidazole, triazole, quinoline, spirooxindole) and activation terms (photoredox, electrochemical, mechanochemical, continuous flow). The reference lists of recent reviews [7-15] were screened in addition.

Studies were included when they met two criteria. First, three or more distinct components react in one pot without isolation of an intermediate; pseudo-multicomponent and sequential one-pot processes are included but labelled as such (Section 2.1). Second, the product is a five- or six-membered nitrogen heterocycle, or a fused or spiro derivative, formed either within the multicomponent step or by a defined post-condensation step. Three- and four-membered nitrogen heterocycles, macrocycles and framework materials are outside the scope. Reactions in which a heterocycle is a reagent rather than a product are not treated as heterocycle syntheses; two such methods are retained in Table **2** as flagged comparators (entries D2 and D3).

From the eligible literature, 24 representative methods were selected for detailed evaluation (Table **2**). They were chosen to cover the entry manifolds, the principal ring classes, the main catalyst types and the photochemical and electrochemical activation modes discussed in Sections 4 to 8, rather than to be exhaustive; counts derived from Table **2** (Fig. **8**) therefore describe this set and not the field as a whole. Every method was assessed on the same three axes: the level of mechanistic evidence (Section 1.2), the recycling tier of any heterogeneous catalyst (R0–R3, Section 6.4), and the mass metrics, with calculated atom economies kept separate from experimentally determined values (Section 9.1 and Table **4**). All assignments are based on the experiments reported in each source.

1.2. Criteria for Grading Mechanistic Evidence

Mechanistic proposals are graded on a three-level scale. The grade records the strongest experimental evidence reported for the pathway that forms the product, and it is assigned to a specific method or manifold rather than to a named reaction in general.

Level A (direct evidence): the key intermediate of the ring-forming sequence, such as an iminium, nitrilium or N-

acyliminium ion or the open-chain adduct that cyclises, has been isolated and shown to convert into the product, or detected in the reacting mixture by spectroscopy or mass spectrometry; or the proposed pathway is supported by kinetic analysis.

Level B (indirect evidence): the pathway is constrained by control experiments only, such as radical traps, two-component sub-reactions, isotope labelling, dark or current-off controls, or time-course sampling that detects stable upstream species, for example an aldehyde formed by dehydrogenation or a chalcone, without examining the ring-forming steps.

Level C (analogy): the pathway is proposed by analogy with related reactions, with no experimental test.

Computational studies are recorded separately and do not change the grade, because a calculated energy profile constrains a mechanism without establishing it. Methods for which the source reports no mechanistic test are marked "—" and are not graded. These definitions are applied without modification in Sections 3, 6 and 7, in Table **2** and in Figs. (**3** and **8**).

2. FUNDAMENTALS AND CLASSIFICATION

2.1. Definitions

Four terms are used inconsistently in this literature and are worth separating. A multicomponent reaction combines three or more distinct components in one pot with no isolation of intermediates. A pseudo-multicomponent reaction uses two or more equivalents of one component. In the classical Hantzsch dihydropyridine synthesis, for example, two equivalents of the β-ketoester supply both halves of the ring; the operational advantages are the same, but the component count overstates the diversity available. A sequential one-pot process adds components in a defined order, sometimes after a change of conditions; it retains the isolation economy but not the simultaneity. Domino, cascade and tandem describe the internal structure of the bond-forming sequence rather than the number of inputs. In a domino process, each step is the direct consequence of the functionality generated in the preceding one [18]. Most MCRs that close a heterocyclic ring are domino processes by this definition, but a domino reaction need not be multicomponent.

A further distinction matters more than the nomenclature and is used throughout this review: whether the nitrogen heterocyclic ring is closed within the multicomponent step, or whether the MCR delivers an acyclic adduct that is cyclised afterwards. The Ugi and Passerini reactions belong to the second category; their products become heterocycles only through a post-condensation transformation [3, 19]. The Hantzsch, Biginelli, GBB, Povarov, van Leusen and azomethine ylide platforms belong to the first (Fig. **1C**).

2.2. Platforms

Table **1** lists the platforms used in the rest of this review, together with the key intermediate, the stoichiometric by-products, and the atom economy of a balanced model reaction. Every equation underlying the table was balanced computationally. The atom economies are therefore theoretical values calculated from the balanced equations rather than quoted from the source papers, and they are comparable across platforms. Three patterns emerge. First, isocyanide-based platforms are the most atom-economical, because the isocyanide carbon is fully incorporated and water is the only by-product: the Ugi four-component reaction reaches 94.9% and the GBB reaction 93.6%. Second, platforms that expel a leaving group are penalised however efficiently they are executed; the van Leusen imidazole synthesis loses the tosyl group (57.4%), and the three-component copper-catalysed azide–alkyne cycloaddition loses a halide salt (69.6%). Third, ammonium acetate, used almost universally in place of ammonia for operational convenience, costs 11–14 percentage points of atom economy relative to ammonia when the two are compared on the same oxidation accounting, because acetic acid leaves the balance as waste.

Fig. (**2**) recasts the same set as a matrix. Its rows are the electrophile through which the components enter, and its columns indicate whether the ring closes in the pot. This classification is used in preference to the conventional division into isocyanide-based and non-isocyanide-based MCRs, because it groups reactions that share mechanistic behaviour and therefore share failure modes.

3. KEY INTERMEDIATES AND MECHANISTIC EVIDENCE

Four manifolds account for most MCR routes to nitrogen heterocycles. Their mechanisms are not equally well established, and the distinction is practical rather than academic: a pathway supported by intercepted intermediates can be optimised rationally, whereas one asserted by analogy cannot. Each manifold is graded below against the criteria of Section 1.2, and the experiment that determines the grade is stated.

3.1. The Nitrilium Fork: Ugi and GBB

Both reactions begin with condensation of an aldehyde and an amine to an imine. The imine is activated to an iminium ion, which is attacked by the isocyanide to give a nitrilium ion. What follows depends on which nucleophile captures that ion. In the Ugi reaction, the carboxylate adds to give an O-acyl imidate, which undergoes the Mumm 1,3-O→N acyl shift to the bis-amide. In the GBB reaction, the ring nitrogen of the 2-aminoazine adds intramolecularly in a 5-exo-dig sense, and a formal 1,3-hydrogen shift aromatises the imidazo[1,2-a]azine [8, 20]. The same intermediate therefore delivers an acyclic product or a fused bicyclic heterocycle depending only on whether an intramolecular nucleophile is present (Fig. **3A**).

The Ugi manifold is **Level A**, because its key intermediates have been detected directly. Charge-tagged reagents allowed the cationic intermediates to transfer from solution to the gas phase and be characterised by electrospray tandem mass spectrometry, and the Mumm rearrangement was additionally examined by ion-mobility measurements and density functional theory [21]. Computational work has since challenged parts of the textbook picture, in particular the

reversibility of the intermediate steps and the nature of the driving force [22]. A combined experimental and theoretical study also showed that the solvent decides between competing product manifolds, α-acyl aminocarboxamides and α-amino amidines [23]. The mechanism is thus well supported but not static.

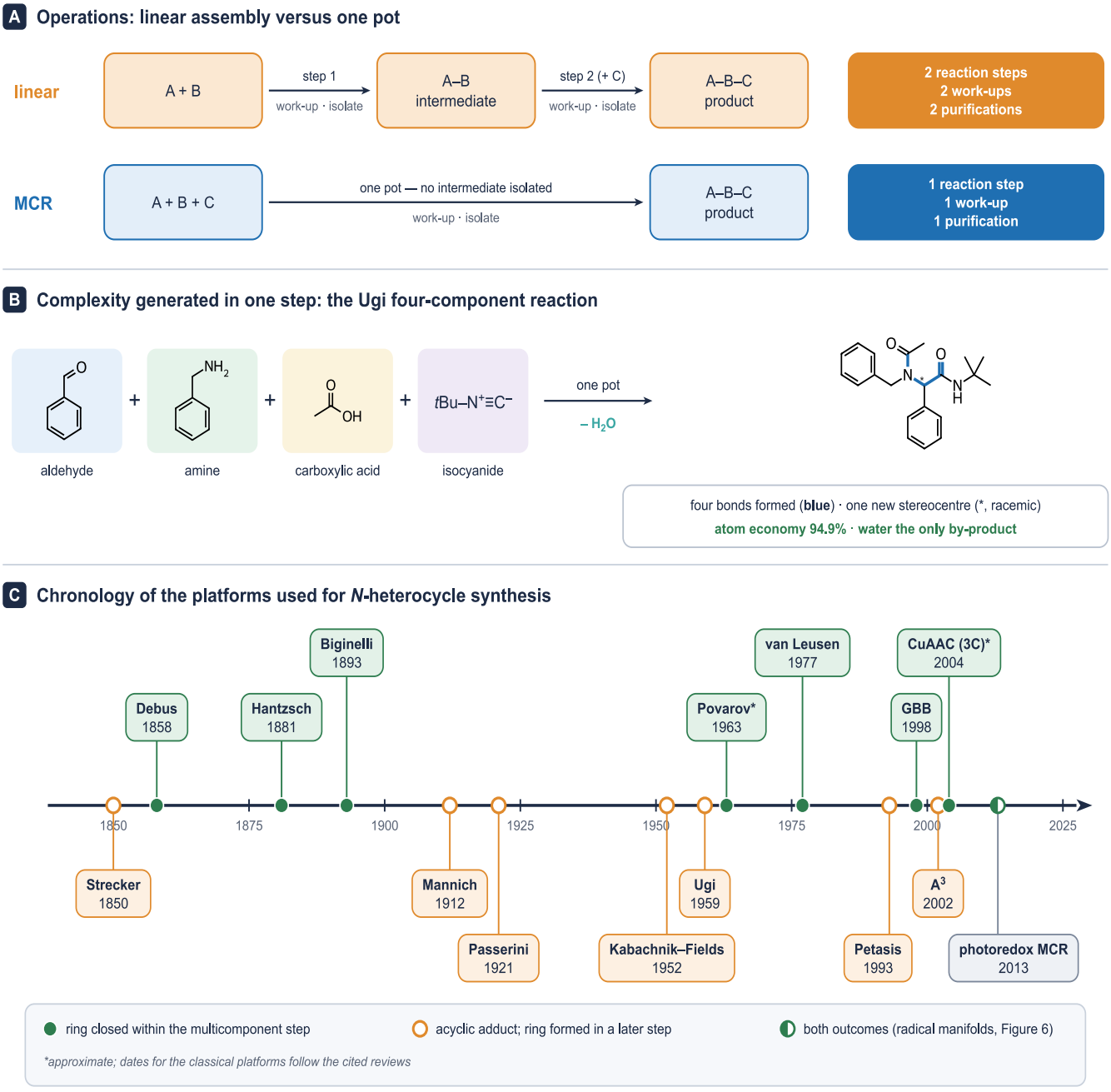


Fig. (1). Multicomponent reactions as a step- and isolation-economic alternative to linear synthesis. (**A**) Unit operations for a linear three-component assembly *versus* a one-pot multicomponent reaction. (**B**) The Ugi four-component reaction of benzaldehyde, benzylamine, acetic acid and tert-butyl isocyanide forms four new bonds (highlighted) and one stereocentre in a single operation, with water as the only stoichiometric by-product; the atom economy (94.9%) is calculated from the balanced equation. (**C**) Chronology of the platforms relevant to nitrogen heterocycle synthesis. Filled markers above the axis denote reactions that close the heterocyclic ring within the multicomponent step, and open markers below the axis denote reactions that give an acyclic adduct, as classified in Table **1**.

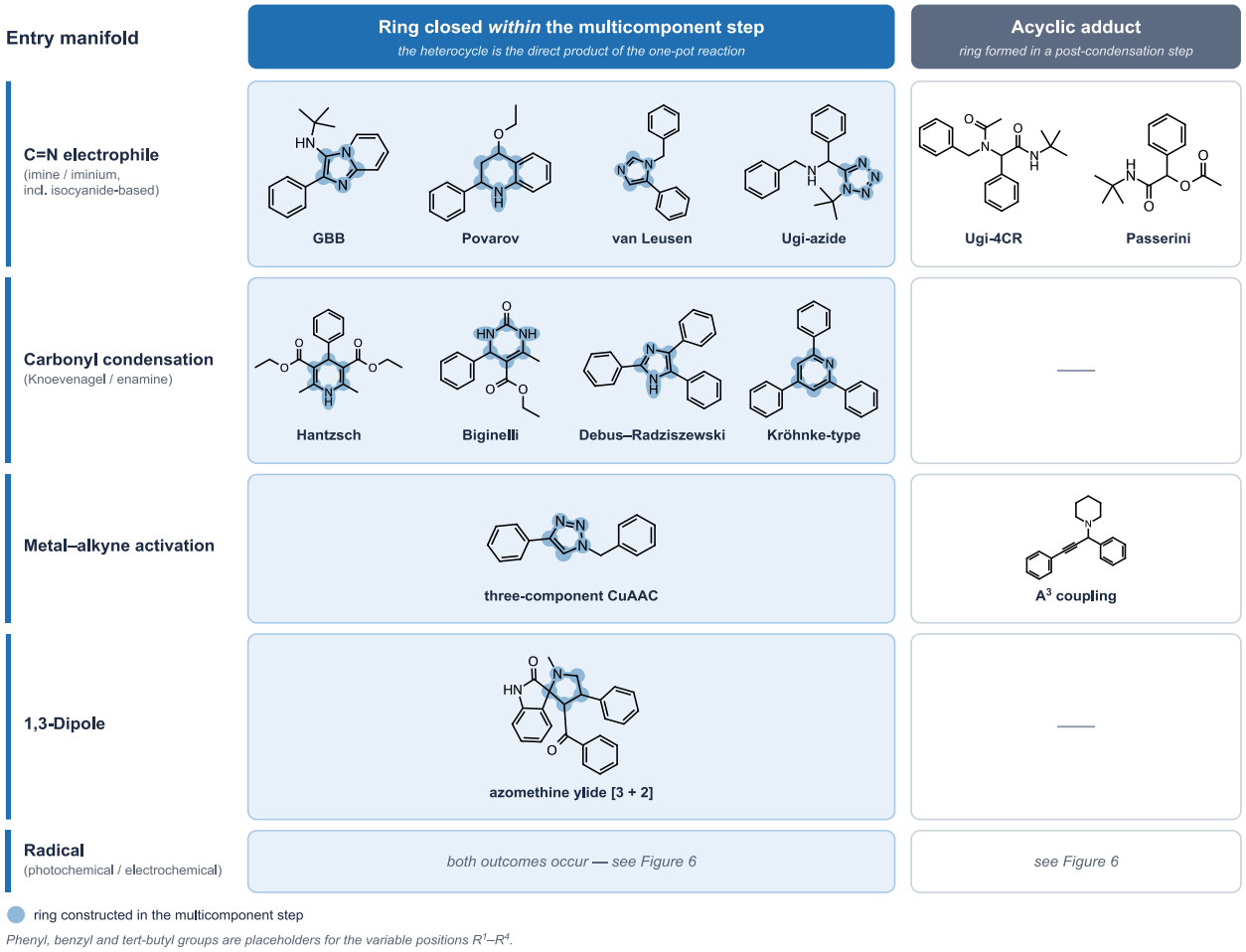


Fig. (2). Classification of MCR platforms by the electrophile through which the components enter the manifold (rows) and by whether the nitrogen heterocycle is closed within the multicomponent step or requires a post-condensation transformation (columns).

The GBB manifold is also **Level A**, on the basis of both mass-spectrometric detection and kinetic analysis, and recent work illustrates how much of the observed reactivity the classical scheme omits [24]. Screening across solvents of varying dielectric constant showed that the uncatalysed reaction proceeds only in methanol and ethanol and fails in water, so bulk polarity alone does not explain the trend. With p-toluenesulfonic acid (10 mol%) in methanol at room temperature, the model reaction of benzaldehyde, 2-aminopyridine and tert-butyl isocyanide reached 94% conversion and 90% isolated yield in six hours [24]. Kinetic modelling showed the reaction to be roughly four times faster in the presence of twenty equivalents of methanol than in its absence. Kamlet–Abboud–Taft analysis identified hydrogen-bond acidity and dipolarity/polarisability, not hydrogen-bond basicity, as the governing descriptors. Charge-tagged ESI-MS monitoring detected the imine and the advanced doubly charged intermediate, together with reversible methanol adducts that are kinetic dead ends. Calculations placed the barrier for the final step implausibly high until a second molecule of 2-aminopyridine was allowed to act as a proton shuttle. This proposal was tested by running the uncatalysed reaction with excess amine, which raised conversion from 40% to 62% [24]. Methanol in this reaction is therefore a co-catalyst rather than an inert medium, a specific instance of the general argument that solvent screening is not the same as understanding solvent effects [15].

3.2. Knoevenagel and Enamine Manifolds: Hantzsch and Biginelli

The Hantzsch dihydropyridine synthesis is conventionally drawn as a convergence of two branches (Fig. **3B**). One is Knoevenagel condensation of the aldehyde with one equivalent of the 1,3-dicarbonyl compound; the other is condensation of the nitrogen source with the second equivalent to an enamine. Michael addition and cyclodehydration then close the ring. No interception study of the Hantzsch reaction is among the sources examined here, so this scheme is shown without an evidence grade. The Biginelli reaction admits three distinct proposals, the iminium, enamine and Knoevenagel

routes, which converge on the same dihydropyrimidinone (Fig. **3C**), and the question of which operates was settled experimentally rather than by argument. Nuclear magnetic resonance monitoring of the classical conditions found no evidence for an initial aldol reaction between the aldehyde and the β-ketoester. Instead, it supported an N-acyliminium ion formed from the aldehyde and urea, intercepted by the β-ketoester to give open-chain ureides that cyclise [25]. Direct-infusion ESI-MS combined with tandem experiments and density functional calculations intercepted cationic intermediates of the iminium route and found none associated with the more demanding Knoevenagel or enamine pathways [26]. The iminium route is therefore **Level A**, with the caveat that the medium matters. In Lewis acid–ionic liquid systems the picture is more complex, because the ionic medium stabilises the charged intermediates, and in an enantioselective variant based on asymmetric counteranion-directed catalysis ESI-MS detected only iminium-route species [27].

The Biginelli literature also supplies the clearest warning about uncritical green labelling. A systematic examination of solvent-free and catalyst-free Biginelli protocols concluded that such claims frequently do not survive scrutiny, and asked directly what the catalysis in these systems is for [28]. That paper should be read alongside any protocol whose novelty rests on the absence of a catalyst.

3.3. The Povarov Manifold

The three-component Povarov reaction of an aniline, an aldehyde and an electron-rich alkene is still frequently described as an imino Diels–Alder cycloaddition. Two recent studies argue against that description on evidence. The first, a study across five Lewis acid catalysts, established experimentally that no product formed in the absence of a catalyst. Its density functional and electron localisation function analysis indicated that the acid is required to generate the iminium ion, and that the sequence proceeds through a Mannich-type adduct followed by intramolecular Friedel–Crafts cyclisation rather than through a concerted transition state [29]. In the second, a mechanochemical enantioselective variant catalysed by a chiral phosphoric acid allowed the addition intermediate to be isolated, and the marked dependence of stereocontrol on the liquid-assisted grinding additive is consistent with a stepwise polar pathway [30]. The manifold is therefore **Level A** on the strength of the isolated addition intermediate [30]. The computational analysis [29] provides support but does not count towards the grade, and the imino Diels–Alder nomenclature is best avoided.

3.4. The Terminal Step, and Where the Evidence Thins

Many MCRs deliver a dihydro intermediate that must be oxidised to the aromatic heterocycle, and this step is where both the mechanistic evidence and the mass balance are weakest (Fig. **3D**). Oxidation of the Hantzsch dihydropyridine with 2,3-dichloro-5,6-dicyano-1,4-benzoquinone (DDQ) has a calculated atom economy of 58.8% for that step alone. Stoichiometrically, this corresponds to 0.69 kg of quinone consumed and 0.70 kg of the derived hydroquinone to dispose of per kilogram of pyridine produced. Aerobic oxidation of the same substrate has a calculated step atom economy of 94.8%, with water as the only by-product. Anodic oxidation removes the chemical oxidant entirely, the electrode serving in its place, at the cost of electrode area and electrolyte.

In practice the terminal step is often left unexamined. Several four-component syntheses of 2-amino-3-cyanopyridines invoke a "vinylogous anomeric-based oxidation" to account for the loss of dihydrogen without identifying the ultimate hydrogen acceptor [31]. This is a **Level C** proposal: it names a pathway without excluding aerial oxidation, disproportionation or oxidation by an excess component, each of which has different implications for the mass balance and for scale-up. The distinction is not pedantic. An unidentified oxidant cannot appear in a balanced equation and therefore cannot appear in an atom economy.

4. SIX-MEMBERED AZINES

4.1. Pyridines

Four families of MCR account for most recent pyridine syntheses, and they differ mainly in which ring positions can be varied independently (Fig. **4A**, **C**). Hantzsch-type assembly gives symmetrical 3,5-disubstituted 1,4-dihydropyridines in which C2 and C6, and C3 and C5, are necessarily identical; only C4 is freely variable. This symmetry constraint is intrinsic to the pseudo-four-component design. It is the main reason the platform survives as a teaching and scaffold-synthesis reaction rather than a library reaction, and catalyst-free protocols in this family remain attractive for exactly that reason [32].

Kröhnke-type condensations of an aldehyde, two equivalents of an aryl ketone and an ammonium source give 2,4,6-triarylpyridines in which C3 and C5 are unsubstituted and C2 and C6 carry the same aryl group. The four-component variant that adds malononitrile is more useful synthetically. The nitrile carbon becomes ring C2, so the amino group at C2 and the nitrile at C3 are installed automatically, leaving C4 and C6 variable. Recent work in this family has focused on the catalyst rather than the disconnection. A Brønsted acidic catalyst prepared by grafting carboxylic acid functionality onto reduced natural asphalt gave 2-amino-3-cyanopyridines in 90–97% yield within 30–50 minutes in water and was recycled over five runs [31]. A layered double hydroxide–supported copper catalyst achieved the same transformation under solvent-free conditions, with recycling over four runs [33].

The Bohlmann–Rahtz synthesis offers the complementary substitution pattern, with variable C2 and C6 and an electron-withdrawing group fixed at C3. Its classical limitation is the requirement for highly reactive aminoacrylates or activated carbonyl partners. Adding ammonium fluoride to cyclic ketones was recently shown to overcome this limitation. Cycloalkane-fused pyridines formed under mild conditions, with selectivity for cyclic over aliphatic ketones, and the method was applied to the natural product epiguaipyridine and to an aza-(5)-helicene [34]. Fused pyridines are also accessible through metal-free oxidative routes: an iodine-mediated three-component reaction of an aminopyrazole, phenylglyoxal monohydrate and phenylhydrazine hydrochloride forms three C–N and two C–C bonds in one operation [35].

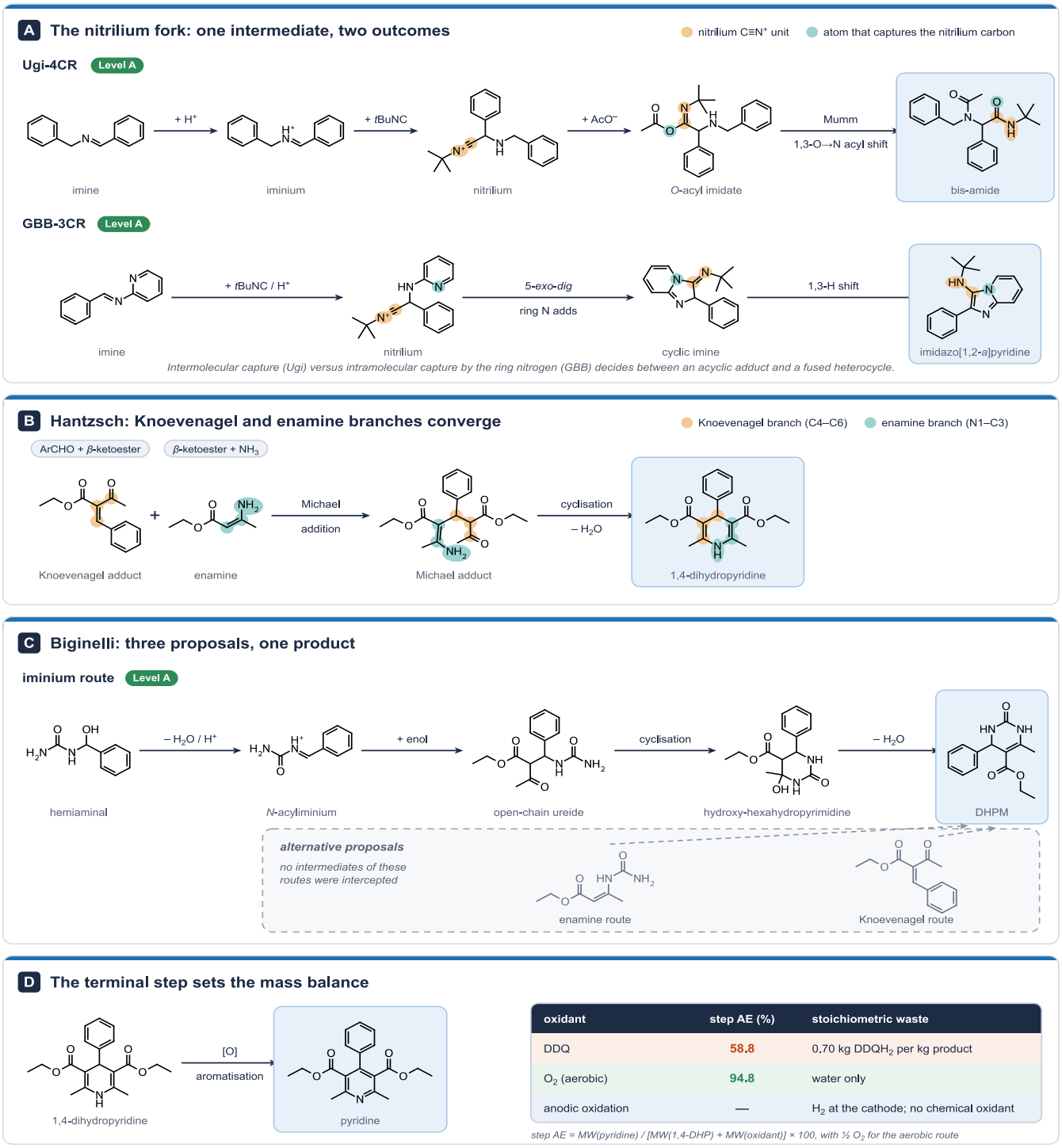
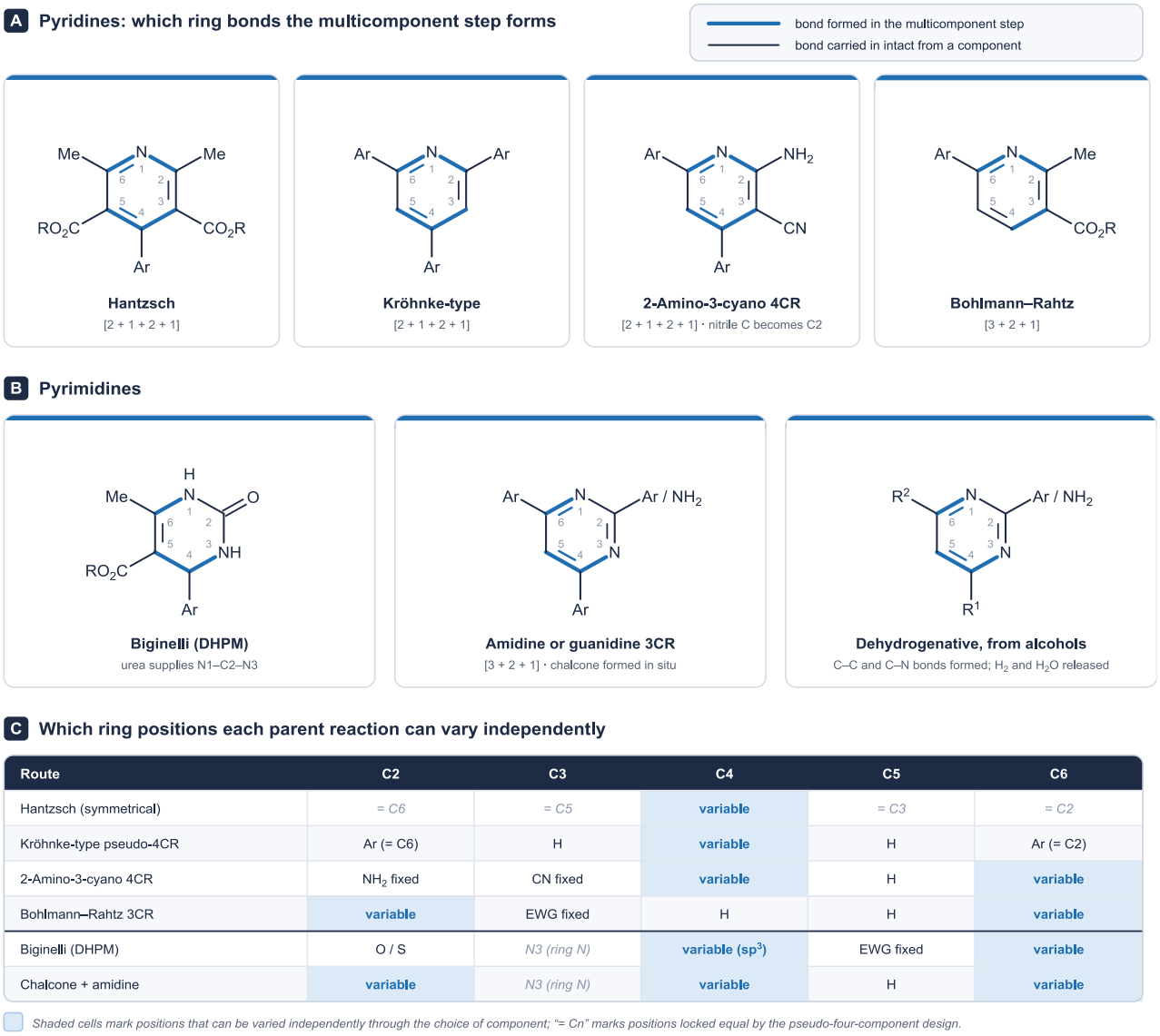


Fig. (3). Recurring mechanistic manifolds and the evidence supporting them. (**A**) Nitrilium ions partition between intermolecular capture followed by Mumm rearrangement (Ugi) and intramolecular capture by a ring nitrogen (GBB). (**B**) The Knoevenagel and enamine branches of the Hantzsch reaction converge at the Michael addition; this scheme is not graded. (**C**) Of the three routes proposed for the Biginelli reaction, only the iminium route has been intercepted experimentally. (**D**) In aromatised products the terminal oxidant, not the multicomponent step, sets the mass balance; step atom economies are calculated values. Evidence levels follow the criteria of Section 1.2.



Route	C2	C3	C4	C5	C6
Hantzsch (symmetrical)	*= C6*	*= C5*	**variable**	*= C3*	*= C2*
Kröhnke-type pseudo-4CR	Ar (= C6)	H	**variable**	H	Ar (= C2)
2-Amino-3-cyano 4CR	NH_2 fixed	CN fixed	**variable**	H	**variable**
Bohlmann–Rahtz 3CR	**variable**	EWG fixed	H	H	**variable**
Biginelli (DHPM)	O / S	*N3 (ring N)*	**variable (sp^3)**	EWG fixed	**variable**
Chalcone + amidine	**variable**	*N3 (ring N)*	**variable**	H	**variable**

Fig. (4). Bond-formation maps for multicomponent routes to pyridines (**A**) and pyrimidines (**B**), with the ring positions each parent reaction can vary independently (**C**). Bonds formed within the multicomponent step are drawn heavy and coloured; bonds carried in intact from a single component are drawn light.

4.2. Pyrimidines

The Biginelli reaction remains the default route to dihydropyrimidinones, and its mechanism is the best characterised in this review (Section 3.2). The more interesting recent development is a different disconnection altogether: the dehydrogenative assembly of pyrimidines from amidines and alcohols (Fig. **4B**). In the original iridium-catalysed version, a PN5P–Ir pincer catalyst combined an amidine and up to three alcohols through alternating condensation and dehydrogenation steps. The condensations deoxygenate the alcohols, and the dehydrogenations aromatise the ring. Thirty-eight pyrimidines were obtained in up to 93% isolated yield, liberating two equivalents of hydrogen and water [36]. Replacing iridium with an earth-abundant metal followed, first with manganese PNP pincer complexes, which additionally allowed β-alkylation to install two different primary alkyl groups and reach fully substituted pyrimidines in one pot [37].

Over the last three years this chemistry has been extended across the first-row metals. Nickel NNS pincer complexes at 3 mol% converted alcohols, malononitrile and guanidine or benzamidine salts into 33 4-aminopyrimidine-5-carbonitriles in up to 95% yield, with water and hydrogen as the only by-products; the protocol was demonstrated on large scale and used in a short synthesis of a cytosine antifungal analogue [38]. A cobalt(III) complex generated *in situ* from common cobalt(II) salts by oxygen activation gave 119 tri- and tetrasubstituted pyrimidines in up to 93% yield from amidines, primary alcohols and aryl ketones, with a further 31 examples

from aliphatic substrates [39]. Nickel NNO pincer complexes at 2 mol% delivered 27 2,4,6-trisubstituted pyrimidines in up to 92% yield on gram scale [40].

Three points of comparison follow. First, on atoms these routes are favourable: the co-products are water and dihydrogen, and the hydrogen is in principle recoverable rather than merely lost, which aromatisation with a stoichiometric oxidant cannot offer. Second, the alcohols are available from lignocellulosic biomass, so the feedstock argument is not merely rhetorical [36]. Third, the constraint has moved from the disconnection to the catalyst. These reactions require a designed pincer ligand, and the mass and step cost of preparing that ligand is not captured by any metric applied to the pyrimidine-forming step itself. This is among the most consequential accounting gaps in the sustainability discussion of Section 9.

5. FIVE-MEMBERED, FUSED AND SPIRO SYSTEMS

5.1. Imidazoles and Imidazo-Fused Azines

The GBB reaction is the most developed isocyanide MCR for fused nitrogen heterocycles. Two decades of work were reviewed comprehensively at its twentieth anniversary, by which point over a hundred patents had been issued and two GBB-derived compounds had received regulatory approval [8]; developments between 2019 and 2023 were surveyed separately [9]. Its value for library synthesis was quantified directly by a parallel-format study. That study compared the two standard protocols, scandium(III) triflate and p-toluenesulfonic acid, across a broad substrate set and found the Lewis acid clearly superior. A 790-member model library was produced with an 85% synthesis success rate, and the validated building blocks were used to enumerate a readily accessible chemical space of 271 million compounds, of which 432 already had recorded biological activity [41]. That 85% figure is a more honest measure of platform scope than any substrate table, and it is unusual for being reported at all.

Related imidazo[1,2-a]pyridines are accessible without isocyanides. A coupled flavin–iodine organocatalytic system formed the C–N bond aerobically from aminopyridines and ketones, and was extended to a one-pot three-step synthesis of 3-thioimidazo[1,2-a]pyridines by adding a thiol [42]. A different kind of input was demonstrated by assembling the same ring system from lignin β-O-4 model compounds and 2-aminopyridine in up to 95% yield, giving access to scaffolds shared with marketed drugs such as zolimidine and alpidem [43]. The van Leusen imidazole synthesis forms 1,5-disubstituted imidazoles from an aldehyde, an amine and a tosylmethyl isocyanide, and it has been adapted to DNA-encoded library synthesis. The validation data are instructive: of 251 aldehydes, 380 amines and 19 tosylmethyl isocyanides tested, 65, 194 and 15, respectively, cleared a 50% yield threshold [44].

5.2. Triazoles

The three-component variant of the Copper-Catalysed Azide–Alkyne Cycloaddition (CuAAC) avoids handling organic azides by generating them *in situ* from an alkyl halide and sodium azide. The chemistry itself is mature, and recent work is catalyst engineering: a silica-coated magnetite-supported copper(0) complex catalysed the reaction in water under mild conditions and was recovered magnetically over eight consecutive runs [45]. As Table **1** shows, the calculated atom economy of this platform is capped near 70% by the halide salt that is necessarily expelled, which no amount of catalyst recycling changes.

5.3. Quinolines, Tetrahydroquinolines and Spirocycles

The Povarov and Doebner reactions have been reviewed recently with an explicit drug-discovery focus [10]. Two directions are worth separating. The first is reagent design that removes a hazard or a constraint. A Povarov-type reaction of anilines with aqueous acetaldehyde and tert-butyl nitrite gave N-nitroso-tetrahydroquinolines without an acid catalyst and without an electron-rich alkene, with the nitroso group serving as a synthetic handle. The products were converted to quinolines, the reaction was demonstrated on gram scale, and the route was applied towards a herbicide candidate and towards montelukast [46]. The second direction is stereocontrol. A chiral phosphoric acid–catalysed three-component vinylogous Povarov reaction using phenolic dienes gave 2,3,4-trisubstituted tetrahydroquinolines in >95:5 dr and up to >99% ee [47]. The mechanochemical variant discussed in Section 3.3 achieved comparable stereocontrol and, by the authors' own mass-intensity comparison, consumed less material than the solution process [30].

Spirooxindoles are assembled by three-component 1,3-dipolar cycloaddition of a dipolarophile with an azomethine ylide, generated *in situ* either from isatin and an amino acid or by α-C–H functionalisation of a cyclic amine. Regio- and diastereoselective access to spirooxindole-pyrrolidines was achieved from a cyclic amine, an aryl aldehyde and an olefinic oxindole [48]; ionic liquids accelerate the classical isatin/amino acid route and act as both medium and catalyst [49]. A variant using vinyl selenones gives spirooxindole-pyrrolizines through cycloaddition followed by spontaneous elimination of benzeneseleninic acid [50]. This is chemically elegant but expels a stoichiometric selenium-containing by-product, a cost that is invisible in the yield and visible only in the atom economy.

6. CATALYTIC STRATEGIES

Rather than listing catalysts by metal, it is more useful to ask what each class is being asked to do, and what evidence supports the claims made for it (Table **3**).

6.1. Generating and Stabilising Cations

The largest class of MCR catalysts exists to form an iminium, N-acyliminium or oxocarbenium ion and to stabilise the charged intermediates downstream. Brønsted acids do this directly: p-toluenesulfonic acid at 10 mol% is the practical optimum for the GBB reaction, outperforming acetic, camphorsulfonic and several mineral acids [24]. Lewis acids do the same through coordination. The comparative study of five Lewis acids in the Povarov reaction quantified the

differences, with indium(III) chloride giving the lowest calculated barrier to iminium formation [29]. Ionic liquids act less as catalysts than as media that stabilise cationic intermediates, which is why the Biginelli mechanism becomes more complex in them [27]. Chiral phosphoric acids extend the same activation mode to enantiocontrol [30, 47], as do chiral anions in asymmetric counteranion-directed catalysis, where the chiral induction and the mechanism were established together by mass spectrometry and calculation [27].

6.2. Transfer Hydrogenation and Acceptorless Dehydrogenation

The pincer complexes of Section 4.2 perform a different function: they dehydrogenate alcohols to carbonyl compounds *in situ* and then remove hydrogen again to aromatise the ring [36, 37]. The shift from iridium to manganese, cobalt and nickel [37- 40] is significant for cost and abundance, but it has introduced a new dependency on elaborate ligands. The mechanistic evidence is generally **Level B** in the sense of Section 1.2: control experiments detect the upstream aldehyde, benzylidenemalononitrile or chalcone intermediates [38, 40], and density functional calculations add separately recorded support in some cases [39].

6.3. Oxidative Organocatalysis and Metal-Free Mediation

Iodine, alone or with a co-catalyst, mediates a substantial share of recent oxidative MCRs. The flavin–iodine system is notable for coupling the two catalysts so that dioxygen is the terminal oxidant [42]. Elsewhere iodine functions stoichiometrically or near-stoichiometrically, and the distinction between a metal-free method and a genuinely catalytic one is worth making explicitly [35].

6.4. Heterogeneous and Recyclable Systems, and How to Judge Them

Supported, magnetic and layered double hydroxide catalysts dominate the recent scaffold-directed literature [31, 33, 45]. Recyclability claims in this area are supported at very uneven levels, and it is useful to grade them: **R0**, not tested; **R1**, yield reported over repeated cycles; **R2**, R1 plus a hot-filtration or split test establishing that catalysis is not homogeneous; **R3**, R2 plus quantified leaching by elemental analysis and post-use characterisation of the recovered solid. The tiers are cumulative, so post-use characterisation without a split or hot-filtration test leaves a claim at R1. Most reports in this set reach R1, with five cycles [31], four cycles [33] and eight runs [45], and the higher tiers are rare. The case for a heterogeneous catalyst rest entirely on its reuse, and preparing these materials consumes reagents and solvent that no reaction-level metric captures. R1 evidence is therefore a weak foundation for a sustainability claim.

6.5. Catalyst-Free Protocols

A substantial subset of MCRs proceeds without an added catalyst, promoted by the solvent, by heat or by one of the components acting as a proton shuttle, as 2-aminopyridine does in the GBB reaction [24]. Such protocols are genuinely attractive when the alternative is a metal that must be removed to pharmaceutical specification. They are also the easiest claim to overstate, and the critical examination of solvent-free and catalyst-free Biginelli protocols [28] is the appropriate standard of proof. A useful precedent for framing the question is the joint analysis of catalysis and solvent effects in the Biginelli reaction, which treated efficiency and sustainability as a single problem rather than attributing the outcome to the absence of a catalyst [51].

7. CHALCONES AS *IN SITU* BIS-ELECTROPHILES

Chalcones occupy an unusual position in this field: they are the products of one of the oldest condensations and the substrates for a large family of heterocyclisations, which makes them a natural hub for multicomponent design (Fig. **5**). When a chalcone is generated in the pot from an aryl aldehyde and an aryl ketone, it presents a Michael acceptor and a ketone to the third component, so that addition, condensation, cyclisation and aromatisation follow in sequence. The distinction that matters for this review is whether the chalcone is formed in the pot, which makes the process a true three-component reaction, or added preformed, in which case the transformation is a two-component cyclocondensation however it is described.

The evidence that these cascades pass through the chalcone now rests on control experiments rather than on analogy. Time-dependent control experiments on the nickel-catalysed dehydrogenative pyrimidine synthesis detected the aldehyde, the ketone and the chalcone in sequence [40], and the copper-catalysed route to pyrazolines and pyrimidines from benzyl alcohols and aryl ketones rests on the same intermediate [52]. Because these experiments detect upstream species but do not examine the ring-forming steps, the chalcone manifold is **Level B** (Section 1.2). It also unifies two literatures that are usually kept apart: the classical chalcone cyclocondensations and the modern acceptorless dehydrogenative couplings differ in how the chalcone is made, not in what happens afterwards.

The calculated atom economies of the model cascades make the trade-offs explicit (Fig. **5**). On a formal dihydrogen-loss basis, with no terminal oxidant in the equation, condensation with guanidine to the 2-aminopyrimidine reaches 86.7%, with thiourea to the dihydropyrimidine-2-thione 88.1%, with phenylhydrazine to the 2-pyrazoline 89.2% and on to the aromatised pyrazole 88.6%, and with hydroxylamine to the isoxazole 85.3%. Entering half an equivalent of dioxygen instead lowers the aminopyrimidine, pyrazole and isoxazole values to 82.1%, 84.6% and 80.4%, so the narrow spread is partly an artefact of leaving the oxidant out. What separates these routes in practice is not the multicomponent step but, once again, the oxidation. Routes that stop at the dihydro level, such as the thiourea cascade, avoid the problem entirely, while those that aromatise inherit whatever oxidant the protocol specifies. The dehydrogenative variants [52] are the cleanest solution, because the hydrogen removed to form the chalcone and the hydrogen removed to aromatise the ring are handled by the same catalytic machinery.

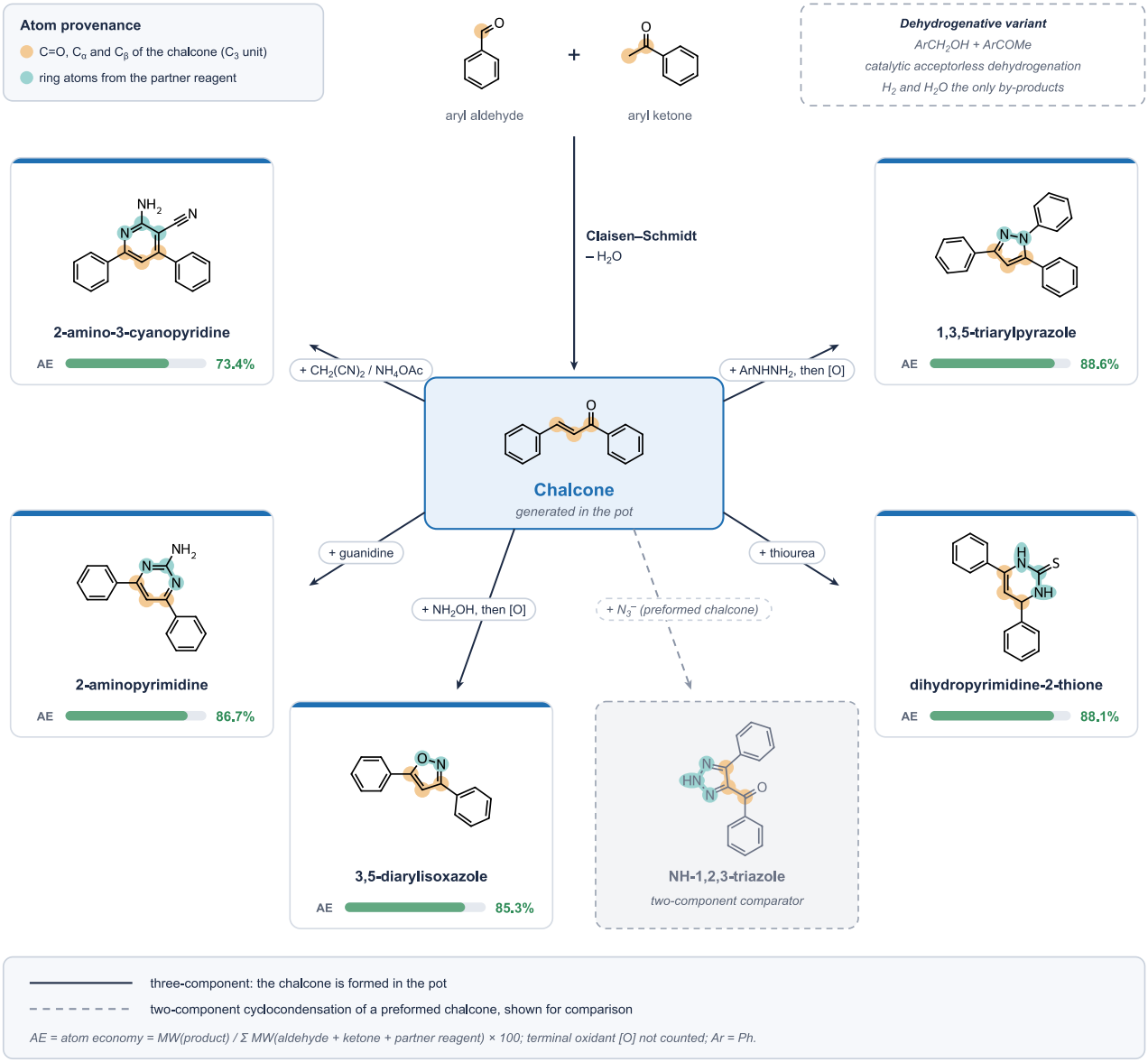


Fig. (5). Chalcones as *in situ* bis-electrophilic intermediates. Solid arrows denote three-component processes in which the chalcone is generated in the pot; the dashed arrow denotes a two-component cyclocondensation of a preformed chalcone, shown for comparison but not counted as a multicomponent reaction. Atom economies are calculated from the balanced model equations on a formal dihydrogen-loss basis; the terminal oxidant is not entered into the equation. For this reason, the 2-amino-3-cyanopyridine value (73.4%) is higher than the 70.4% given in Table **1** and Fig. **7A**, where ½ O_2 is entered as the oxidant.

8. PHOTOCHEMICAL AND ELECTROCHEMICAL MULTICOMPONENT REACTIONS

Light and current entered MCR chemistry as ways of generating radicals under mild conditions (Figs. **6A-C**). The field has been reviewed thoroughly from the standpoint of atom and energy economy [11] and, more recently, at the intersection of the two activation modes [12]. Since the early demonstrations of visible-light photoredox-catalysed MCRs [53], the number of reports has grown quickly, and the useful question is no longer whether such reactions work but what they add.

Three outcomes should be distinguished (Fig. **6D**). The first is a genuinely new disconnection: a component that cannot be introduced thermally. The second is the removal of a catalyst or an oxidant. A visible-light three-component synthesis of isoxazolines and isoxazoles, for example, proceeds through *in situ* nitronate formation and [3+2] cycloaddition at room temperature without a metal and without a photocatalyst [54], which is a real simplification over the

thermal alternatives. The third, and the most common in practice, is the substitution of photochemical for thermal activation in a sequence that already worked. Reports in the third category are often presented as advances in multicomponent synthesis when they are in fact advances in functionalisation. A visible-light halogen-atom-transfer protocol that hydroxyacetylates an existing imidazo[1,2-a]pyridine is a three-component reaction, but it does not build the ring [55]. Similarly, an electrochemical three-component aminoselenation in which an azole is a reagent rather than a product is a difunctionalisation of a diene [56]. Both are useful chemistry; neither is a multicomponent heterocycle synthesis, and conflating the two inflates the apparent scope of the field.

The practical criteria for evaluating a light- or current-driven MCR are therefore narrow and testable (Fig. **6D**). Does a dark control or a current-off experiment fail? Is a quantum yield or a current efficiency reported? Is the ring formed in the step being described? Does the photon flux or electrode area scale with the batch? The last is the binding constraint on scale-up and is the main reason flow photochemistry rather than batch appears in the outlook of this field.

9. SUSTAINABILITY MEASURED

9.1. Calculated and Experimentally Determined Metrics

Two kinds of number appear in this section, and they answer different questions. Calculated, or theoretical, values are obtained from a balanced equation alone. They include the atom economy of a reaction, the step atom economy of an oxidation, and stoichiometric waste masses such as the 0.69 kg of DDQ consumed per kilogram of pyridine. Because they assume complete conversion, exact stoichiometry and no solvent, they set a ceiling on material efficiency but say nothing about how a reaction was actually run. Experimentally determined values require the masses actually charged and isolated. Reaction mass efficiency combines atom economy with the isolated yield and any excess of reagents [16], and process mass intensity and the E factor add solvent, work-up and purification [16, 17].

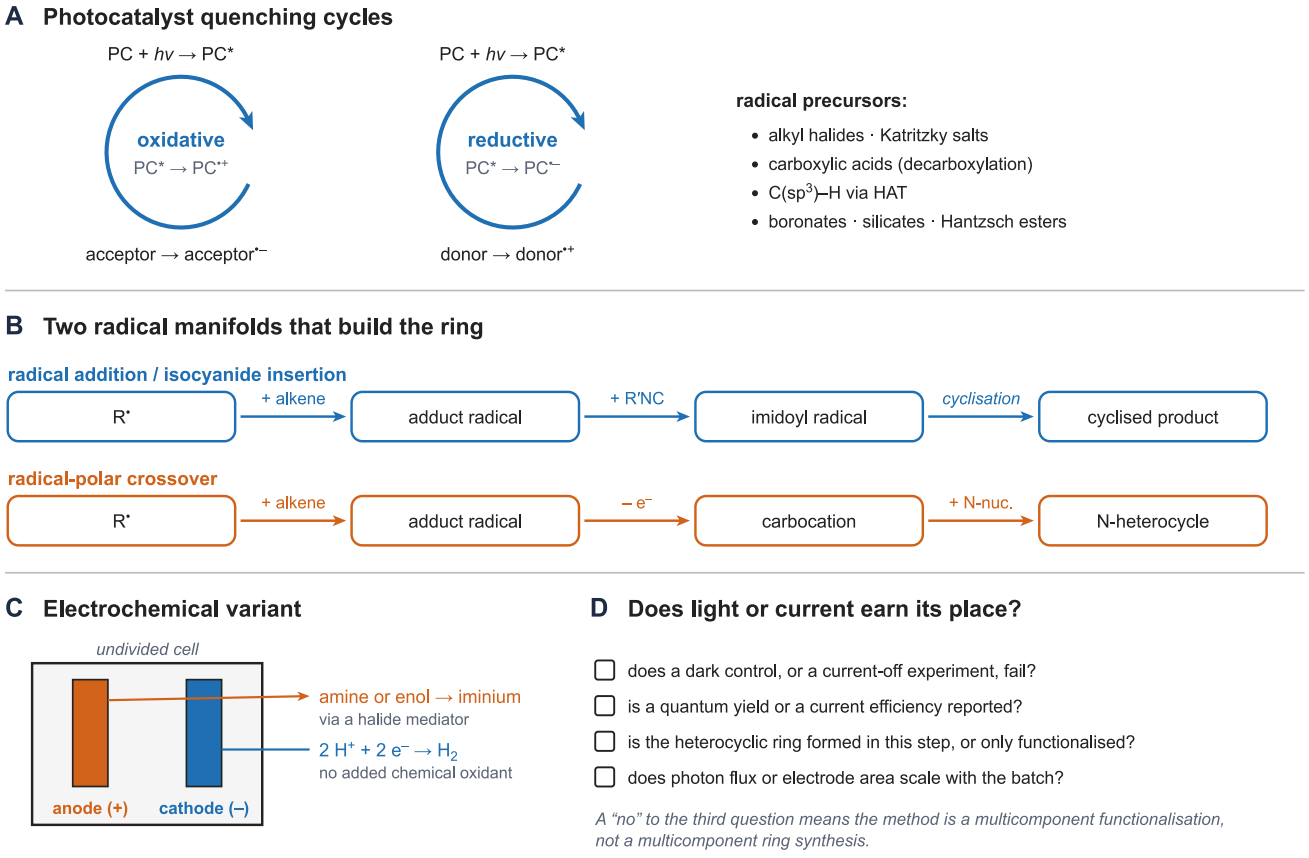


Fig. (6). Photochemical and electrochemical entry points into multicomponent nitrogen heterocycle synthesis. (**A**) Oxidative and reductive quenching cycles of a photocatalyst (PC) and common classes of radical precursor. (**B**) An undivided cell in which the electrophile, an iminium ion, is generated anodically, directly or through a halide mediator, and protons are reduced at the cathode. (**C**) Two radical manifolds that build the ring: radical addition with isocyanide insertion, and radical–polar crossover. (**D**) Criteria for evaluating a light- or current-driven MCR (Section 8) and the three possible outcomes; methods that only functionalise a preformed ring are not counted as multicomponent heterocycle syntheses.

Every atom economy in this review, in Tables **1** and **4** and in Figs. (**3D**, **5** and **7**), is a calculated value from a balanced model equation. No RME or PMI value has been calculated here from primary data, because the charged masses and purification inventories are rarely reported in a comparable form (Section 9.3); the only experimentally based mass-intensity comparison discussed is the one made by the original authors within a single study [30]. Where a source reports an isolated yield, the two kinds of value can be linked, but only as a bound. For the GBB model reaction, the calculated atom economy is 93.6% and the reported isolated yield is 90% [24]. With exactly stoichiometric charging, RME could therefore not exceed about 84% (0.936 × 0.90). Any excess of a component lowers it further, and methanol, although it acts as a co-catalyst, enters PMI but not RME. The 84% figure is thus an upper bound derived from one calculated and one experimental quantity, not a measured RME.

9.2. What Atom Economy Does and Does not Capture

Atom economy is the only mass metric that can be calculated from a balanced equation without knowing how a reaction was run, which is why it is quoted so often and why it is insufficient. Three conclusions follow from the calculated values in Table **1** and Fig. (**7**). First, the differences between MCR platforms are modest, with most values between 85% and 95%, so atom economy does not discriminate usefully among them. Second, the nitrogen source is a larger variable than the platform. When each pair is computed on the same oxidation accounting, replacing ammonia with ammonium acetate costs 11.6 percentage points in the Hantzsch reaction, 11.1 in the Kröhnke-type cascade and 14.3 in the 2-amino-3-cyanopyridine cascade, because the acetate leaves as acetic acid. Third, where an aromatic product is formed from a dihydro precursor, it is the identity of the terminal oxidant rather than the multicomponent step that sets the mass balance. Quinone oxidation drops the step atom economy to 58.8% and puts 0.69 kg of quinone into the balance per kilogram of product, whereas aerobic oxidation of the same substrate gives 94.8%.

What atom economy does not see is everything that is not a reagent atom: the excess of one component used to push the equilibrium, the solvent, the aqueous work-up, and the silica and eluent consumed in purification. In pharmaceutical practice these dominate, which is why process mass intensity is the metric used to drive process improvement [17], and why the E factor was refined to distinguish simple from complete accounting [16].

9.3. An Audit Protocol

The primary literature surveyed here reports atom economy occasionally and reaction mass efficiency or process mass intensity almost never. Where a comparison is attempted, it is generally within one paper, as in the mass-intensity comparison between the mechanochemical and solution-phase Povarov reactions [30], which is a model for how such claims should be made. To allow cross-paper comparison, Table **4** defines a single protocol and states which quantities are calculated and which are experimental. Atom economy is the only calculated quantity. It is taken from the balanced equation including any stoichiometric oxidant or, where the source does not identify the oxidant, on a formal dihydrogen-loss basis labelled as such. The remaining quantities are experimental and must be computed from the masses reported in the source, normally in the supporting information. Reaction mass efficiency uses the masses actually charged; PMI(reaction) covers reagents, catalyst and reaction solvent per unit mass of isolated product; PMI(total) adds work-up, drying agents, silica and eluent, and recrystallisation solvent; and the complete E factor is PMI(total) − 1 [16]. Solvents are classified against a published selection guide [57] rather than described as green or otherwise. Energy input is recorded qualitatively, because mass metrics do not capture it and because microwave, ultrasound, photochemical and electrochemical protocols differ enormously in this respect.

Applying this protocol exposes three hotspots that recur across the methods reviewed here. The first is the stoichiometric oxidant, already discussed. The second is purification: a reaction run neat in ten minutes and then purified by column chromatography has a PMI dominated by the silica and eluent, and the solvent-free label describes only the first step. The third is catalyst provenance. A designed pincer ligand [36-40] or a functionalised magnetic support [45] consumes reagents, solvent and synthetic steps before the MCR begins. Unless the catalyst is recycled enough times to amortise that cost, and unless the recycling evidence rises above tier R1, the accounting boundary has simply been drawn to exclude the expensive part.

9.4. Where the Genuine Gains Are

Three strategies survive this scrutiny. Acceptorless dehydrogenative coupling is a particularly compelling case: it replaces a stoichiometric oxidant with catalytic hydrogen removal, releases water and dihydrogen rather than reduced quinone or metal salts, and starts from alcohols rather than pre-oxidised carbonyl compounds [36-40, 52]. Mechanochemistry is the second, where the comparison is made within the same study and the improvement in mass intensity is measured rather than asserted [30, 58]. Continuous flow is the third, both because it removes the batch constraint on photochemical and high-temperature steps and because it tends to reduce solvent inventory. A multicomponent flow process to fused imidazoheterocycles was developed explicitly on those grounds [59], and the broader case has been reviewed [60]. In each of these, the sustainability claim is tied to a measurable quantity rather than to the one-pot format itself.

10. MEDICINAL CHEMISTRY RELEVANCE

The medicinal value of MCR-derived heterocycles is best demonstrated by specific compounds rather than by activity lists. Monastrol, a dihydropyrimidinethione accessible by the Biginelli reaction, was identified in a phenotype-based screen as an inhibitor of the mitotic kinesin Eg5. It was the first small molecule shown to perturb the mitotic machinery without targeting tubulin [61], and it remains the standard illustration that a Biginelli scaffold can address a target class that resisted conventional chemotypes.

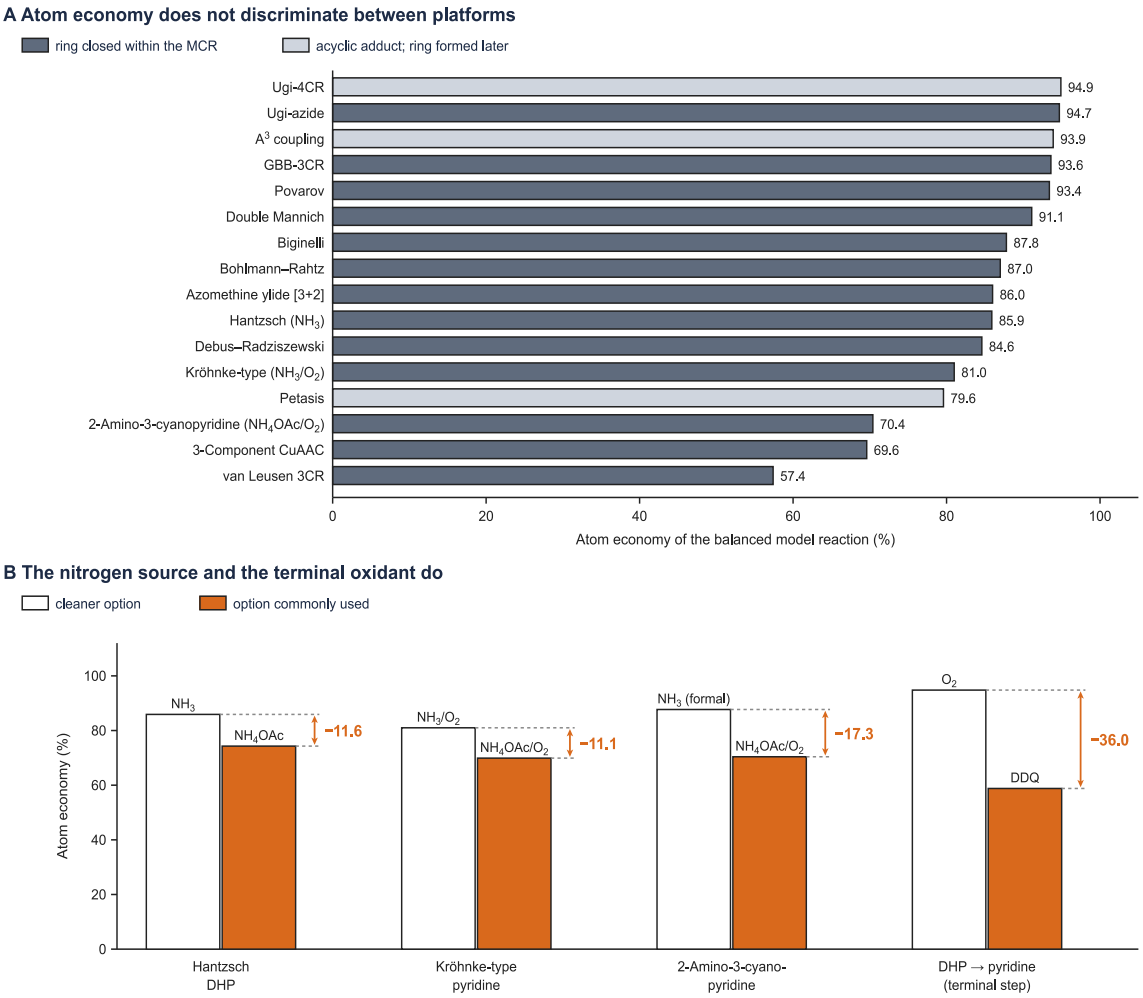


Fig. (7). Atom economies calculated from balanced model equations. (**A**) Platforms ranked by atom economy; 10 of the 16 values fall between 85% and 95%, so atom economy alone does not discriminate between them. (**B**) The two variables that do: the nitrogen source and the terminal oxidant. Each pair is compared on the same oxidation accounting, stated beneath it. Replacing ammonia with ammonium acetate costs 11.6, 11.1 and 14.3 percentage points in the three models. For the 2-amino-3-cyanopyridine pair, both values are on a formal dihydrogen-loss basis (87.7% and 73.4%), whereas the 70.4% in panel A and Table **1** includes ½ O_2. 2,3-Dichloro-5,6-dicyano-1,4-benzoquinone (DDQ) costs 36.0 percentage points relative to dioxygen and places 0.69 kg of quinone and 0.70 kg of the derived hydroquinone in the waste stream per kilogram of pyridine. All values in this figure are theoretical atom economies, not measured reaction mass efficiencies or process mass intensities.

Three more recent examples show the pattern that makes MCRs valuable in discovery: a scaffold hypothesis, a one-step synthesis and rapid structural validation. In the first, a hydrazine fragment was proposed as a multivalent warhead for the aspartic acid pair in aspartyl protease active sites. It was incorporated into a multicomponent reaction to enumerate a large virtual library of one-step-accessible hydrazine-tetrazoles, which was screened by anchor-based pharmacophore matching, and the top-ranked compounds were resynthesised and confirmed by enzyme assay and soaked crystal structures [62]. In the second, imidazopyridines, the GBB scaffold class, have been developed as PD-1/PD-L1 antagonists; the reported candidates bind PD-L1 with low-micromolar affinity in biophysical assays, and the binding mode was defined by a co-crystal structure [63]. In the third, a Povarov–Doebner multicomponent reaction gave HSKB142, an orally bioavailable 3H-pyrazolo[4,3-c]quinoline that suppresses type-I interferon expression in human THP-1 monocytes stimulated with 2'3'-cGAMP and is non-cytotoxic to immune cells [64]. At the platform level, two GBB-derived compounds have received regulatory approval [8].

The natural extension is DNA-encoded library technology, where the one-pot format and the aqueous, DNA-compatible conditions align well. Both the GBB reaction [65] and the van Leusen imidazole synthesis [44] have been adapted to this setting, and the associated building-block validation data are among the few sources of honest, large-scale scope statistics in the MCR literature.

Table 1. Multicomponent platforms for nitrogen heterocycle synthesis.

Atom economies are theoretical values calculated here from balanced model equations (benzaldehyde, acetophenone, ethyl acetoacetate, benzil, tert-butyl isocyanide and the corresponding parent nitrogen sources); every equation was balanced computationally before the value was taken. Values are therefore comparable across rows, are not quoted from the source papers, and are not experimental reaction mass efficiencies.

Platform	Components (Model)	Key Intermediate	Ring Closed in MCR?	Products	Stoichiometric by-Products	Calculated AE (%)
Hantzsch	ArCHO + 2 β-ketoester + NH_3	Knoevenagel adduct + enamine	Yes	1,4-Dihydropyridines → pyridines	3 H_2O (+ AcOH)	85.9 (NH_3) 74.3 (NH_4OAc)
Biginelli	ArCHO + β-ketoester + urea	N-Acyliminium	Yes	Dihydropyrimidinones	2 H_2O	87.8
Kröhnke-type pseudo-4CR	ArCHO + 2 ArCOMe + NH_4OAc + [O]	Chalcone → 1,5-diketone	Yes	2,4,6-Triarylpyridines	4 H_2O (+ AcOH)	81.0 (NH_3/O_2) 69.9 (NH_4OAc/O_2)
2-Amino-3-cyanopyridine 4CR	ArCHO + ArCOMe + $CH_2(CN)_2$ + NH_4OAc + [O]	Knoevenagel or Michael adduct (disputed)	Yes	2-Amino-3-cyanopyridines	3 H_2O (+ AcOH)	70.4 (NH_4OAc/O_2)
Bohlmann–Rahtz 3CR	β-Ketoester + NH_3 + alkynone	Enamine → aminodienone	Yes	2,3,6-Trisubstituted pyridines	2 H_2O	87.0
Debus–Radziszewski	1,2-Diketone + ArCHO + 2 NH_3	Diimine (proposed)	Yes	2,4,5-Triarylimidazoles	3 H_2O	84.6
van Leusen 3CR	ArCHO + amine + TosMIC	Imine + TosMIC anion	Yes	1,5-Disubstituted imidazoles	H_2O + TsH	57.4
GBB-3CR	2-Aminoazine + ArCHO + isocyanide	Nitrilium → 5-exo-dig	Yes	Imidazo[1,2-a]azines	H_2O	93.6
Povarov	$ArNH_2$ + ArCHO + electron-rich alkene	N-Aryl iminium (stepwise)	Yes	Tetrahydroquinolines	H_2O	93.4
Ugi-azide	ArCHO + amine + HN_3 + isocyanide	Nitrilium → azide	Yes	1,5-Disubstituted tetrazoles	H_2O	94.7
Three-component CuAAC	RX + NaN_3 + terminal alkyne	Copper acetylide	Yes	1,4-Disubstituted 1,2,3-triazoles	NaX	69.6
Azomethine ylide [3+2]	Isatin + sarcosine + enone	Azomethine ylide	Yes	Spiropyrrolidine oxindoles	CO_2 + H_2O	86.0
Double Mannich	2 ArCHO + NH_3 + acetonedicarboxylate	Iminium / enol	Yes	4-Piperidones	2 H_2O	91.1
Ugi-4CR	ArCHO + amine + acid + isocyanide	Nitrilium → Mumm	No (post-condensation)	Bis-amides → diketopiperazines, benzodiazepines	H_2O	94.9
A^3 coupling	ArCHO + amine + terminal alkyne	Iminium + metal acetylide	In-pot cyclisation only	Propargylamines	H_2O	93.9
Strecker / Passerini / Kabachnik–Fields / Petasis	—	Iminium / nitrilium	No	Acyclic adducts	H_2O / none / $B(OH)_3$	79.6–100

Table 2. Representative multicomponent routes to nitrogen heterocycles, 2019–2026.

Evidence levels A–C as defined in Section 1.2; "—" indicates that the source does not report a mechanistic test. Computational support is noted but does not change the level. Recycling tiers R0–R3 as defined in Section 6.4. Entries marked † report scope and yield ranges but not the full temperature/time profile in the abstract; these are cited for the disconnection and the catalytic strategy rather than for optimised conditions.

#	Heterocycle	Components / Disconnection	Catalyst and Medium	Reported Scope and Key Observation	Evidence	Ref.
A1	1,4-DHPs	Hantzsch 4-CR (aldehyde, 2 β-ketoester, N source)	Catalyst-free	Teaching-lab protocol; full conditions to extract†	—	[32]
A2	Bis-pyrazolo-fused pyridines	Aminopyrazole + phenylglyoxal hydrate + $PhNHNH_2 \cdot HCl$	I_2-mediated, metal-free	3 C–N + 2 C–C bonds formed in one pot†	B	[35]
A3	Cycloalkane-fused pyridines	Modified Bohlmann–Rahtz: propargyl ketone + cyclic ketone + NH_4F	NH_4F-mediated; mild conditions	Selective for cyclic over acyclic ketones; natural-product application†	—	[34]
A4	2-Amino-3-cyanopyridines	ArCHO + ketone + $CH_2(CN)_2$ + NH_4OAc (enone-type)	Asphalt-derived $–CO_2H$ catalyst, water	90–97% in 30–50 min; ≥5 cycles (R1)†	C	[31]
A5	2-Amino-3-cyanopyridines	ArCHO + ArCOMe + $CH_2(CN)_2$ + NH_4OAc (enone-type)	LDH-supported Cu, solvent-free	4 cycles (R1)†	—	[33]
A6	Pyrimidines	Amidine + primary alcohol + secondary alcohol (dehydrogenative)	Ru(II) 2-(2-benzimidazolyl)pyridine complex	Highly substituted pyrimidines; ligand cooperation supported by control experiments†	B	[66]
A7	Trisubstituted pyrimidines	Alcohol + alkyne + amidine (dehydrogenative)	Phosphine-free Fe arylazo pincer, air	Earth-abundant metal; mild aerobic conditions†	—	[67]
A8	4-Aminopyrimidine-5-carbonitriles	Alcohol + $CH_2(CN)_2$ + guanidine/benzamidine	Ni(II)–NNS pincer, 3 mol%	33 examples, ≤95%; scale-up†	B	[38]
A9	2,4,6-Tri/2,4,5,6-tetrasubstituted pyrimidines	ArCOMe + primary alcohol + amidine (enone-type)	Co(III) complex formed *in situ*	119 + 31 examples, ≤93%; control + DFT†	B	[39]
A10	2,4,6-Trisubstituted pyrimidines	Primary alcohol + 1-phenylethanol + amidine/guanidine	Ni(II)–NNO pincer, 2 mol%	27 examples, ≤92%; chalcone intermediate detected; gram scale†	B	[40]
B1	Fused imidazo-heterocycles	GBB-3CR in continuous flow	Acid-catalysed, flow	Sustainability and scale claims to audit (Table **4**)†	—	[59]
B2	Imidazo[1,2-a]pyridines	GBB-3CR: 2-aminopyridine + ArCHO + tBuNC	PTSA 10 mol%, MeOH, rt, 6 h	Model 94% conv., 90% isolated (6 h); MeOH acts as co-catalyst†	A	[24]
B3	Imidazo[1,2-a]pyridines (+3-thio)	Aminopyridine + ketone (+ thiol)	Flavin–I_2 dual organocatalysis; O_2 terminal oxidant	Aerobic C–N/C–S formation†	—	[42]
B4	1,5-Disubstituted imidazoles	van Leusen 3-CR on solid phase/DNA	DNA-compatible conditions	251 aldehydes, 380 amines, 19 TosMICs validated†	—	[44]
B5	1,4-Disubstituted 1,2,3-triazoles	RX + NaN_3 + terminal alkyne	Fe_3O_4@SiO_2-supported Cu(0), water	≤8 runs (R1; ICP characterisation reported)†	—	[45]
B6	N-Nitroso-THQs → quinolines	Aniline + aq. MeCHO + tBuONO	Acid- and alkene-free Povarov-type	Gram scale; route towards montelukast†	—	[46]

B7	2,3,4-Trisubstituted THQs	Vinylogous Povarov 3-CR	Chiral phosphoric acid	>95:5 dr, up to >99% ee†	—	[47]
B8	THQs	Povarov 3-CR under ball milling (LAG)	Chiral BINOL-phosphoric acid (TRIP)	Lower mass intensity than solution; addition intermediate isolated†	A	[30]
B9	Spirooxindole-pyrrolidines	THIQ + ArCHO + olefinic oxindole ([3+2])	Azomethine ylide *via* α-C–H functionalisation	Regio- and diastereoselective†	—	[48]
B10	Spirooxindole-pyrrolizines	α-Amino acid + isatin + vinyl selenone ([3+2]/elimination)	Mild conditions	Stoichiometric PhSe(O)OH released (AE penalty)†	—	[50]
C1	1,3,5-Pyrazolines; 2,4,6-pyrimidines	$ArCH_2OH$ + ArCOMe + $PhNHNH_2$ or amidine (*in situ* chalcone)	NNN–Cu(II), acceptorless dehydrogenation	30 + 37 examples, ≤94%; H_2O/H_2 by-products†	B	[52]
D1	Isoxazolines/isoxazoles	*In situ* nitronate + alkene/alkyne ([3+2])	Visible light, metal- and catalyst-free, rt	Photo-MCR without photocatalyst†	—	[54]
D2	Hydroxyacetylated imidazo[1,2-a]pyridines	Imidazopyridine + diazo ester + I_2 (air)	Visible-light XAT; no photocatalyst	Functionalises a preformed ring (flag: not ring-forming)†	—	[55]
D3	Se-allyl azoles	1,3-Diene + azole + diselenide	Electrochemical	Azole is a component, not a product (flag)†	—	[56]

Table 3. Catalytic strategies, by function.

Class	Function in the Manifold	Representative Systems	Principal Liability	Recycling Tier	Refs
Brønsted acids	Iminium/N-acyliminium formation; stabilisation of cationic intermediates	PTSA (10 mol%, MeOH); AcOH, CSA, sulfonic acids	Substrate acid sensitivity; limited stereocontrol	n/a	[24]
Lewis acids	Carbonyl activation; iminium generation	$InCl_3$ and related acids (Povarov); $Sc(OTf)_3$ (GBB)	Moisture sensitivity; metal removal	n/a	[29, 41]
Chiral phosphoric acids	Enantiocontrol in cation-based manifolds	BINOL-derived TRIP; vinylogous Povarov catalysts	Catalyst cost; narrow substrate windows	n/a	[30, 47]
Chiral anions / ionic liquids	Stabilisation of charged intermediates; asymmetric counteranion-directed catalysis	Chiral task-specific ionic liquids (Biginelli)	Medium cost; viscosity; recovery	R0–R1	[27, 49]
Ir / Mn pincer complexes	Acceptorless dehydrogenation of alcohols and terminal aromatisation	PN5P–Ir; PNP–Mn	Ligand synthesis cost; high temperature	R0	[36, 37]
Ni / Co / Cu pincer and chelate complexes	As above, with earth-abundant metals	Ni–NNS (3 mol%); Ni–NNO (2 mol%); Co(III) formed *in situ*; Cu(II)–NNN	Ligand synthesis cost; mechanism mostly Level B	R0–R1	[38-40, 52]
Iodine and coupled organocatalysis	Oxidative C–N/C–S bond formation; terminal aromatisation	Flavin–I_2 with O_2 as terminal oxidant; I_2/DMSO systems	Often stoichiometric in practice; iodinated waste	n/a	[35, 42]
Supported, magnetic and layered materials	Brønsted or Lewis acid sites on a recoverable solid	Carboxylate-functionalised reduced asphalt oxide; LDH-supported Cu; Fe_3O_4@SiO_2–Cu(0)	Preparation cost excluded from reaction metrics; leaching seldom quantified	R1 (5, 4 and 8 cycles respectively)	[31, 33, 45]
Catalyst-free / solvent-promoted	Solvent or component acts as proton shuttle or co-catalyst	MeOH in GBB; 2-aminopyridine as shuttle; neat thermal Biginelli	Claims frequently overstated; see critical analysis	n/a	[24, 28, 32]

Table 4. Mass-metric audit: protocol and calculated atom economies.

Atom economy is the only calculated (theoretical) quantity in this table; it is taken from the balanced model equation, including any stoichiometric oxidant. Reaction mass efficiency and process mass intensity are experimental quantities: they require the masses actually charged and the purification inventory, which are reported in the supporting information of the primary papers rather than in their main texts. The column on experimental data records what each source makes available; no RME or PMI value has been calculated here. PMI(reaction) covers reagents, catalyst and reaction solvent per unit mass of isolated product; PMI(total) adds work-up, drying agents, chromatographic silica and eluent, and recrystallisation solvent; the complete E factor is PMI(total) − 1. Solvents are classified against a published selection guide rather than described as green.

Entry	Transformation (Model)	Calculated AE (%)	Experimental Data in Source (RME, PMI)	Principal Mass Hotspot	Assessment
Nitrogen source	Hantzsch 4CR with NH_3 vs NH_4OAc	85.9 / 74.3	AE only	Acetic acid expelled from NH_4OAc	Choice of nitrogen source costs 11.6 points here, and 11–14 points across the models of Fig. (**7B**), before any process consideration
Terminal oxidant	1,4-Dihydropyridine → pyridine, DDQ vs O_2	58.8 / 94.8	AE only	0.69 kg DDQ and 0.70 kg hydroquinone per kg product	The oxidant, not the MCR, sets the mass balance wherever aromatisation needs a stoichiometric oxidant
Leaving group	van Leusen 3CR; three-component CuAAC	57.4 / 69.6	AE only	Sulfinate; halide salt	Intrinsic ceiling; not improvable by catalyst or solvent choice
Isocyanide platforms	Ugi-4CR; GBB-3CR	94.9 / 93.6	AE; solvent and loading reported [24]	Methanol inventory; chromatography	Highest atom economies in the set; purification dominates the true PMI
Chalcone cascades	*In situ* chalcone + guanidine / thiourea / $PhNHNH_2$ / NH_2OH	86.7 / 88.1 / 89.2 / 85.3	AE only	Terminal oxidation in the aromatising cascades	Narrow spread on a formal H_2-loss basis (80–85% with O_2 entered); the differentiator is the oxidation, not the cyclisation
Dehydrogenative coupling	Amidine + alcohols → pyrimidine [36-40]	Not calculable as a single equation (catalytic H_2 release)	Scope and loading reported; charged masses in SI	Pincer ligand synthesis, excluded from reaction-level metrics	Particularly compelling case: H_2O and H_2 as by-products, alcohols as feedstock; catalyst provenance is the open cost
Mechanochemistry	Povarov 3CR, ball milling vs solution [30]	93.4 (model)	Mass intensity compared within the study	Liquid-assisted grinding additive	Measured improvement within a single study; the appropriate standard of proof
Flow	GBB-type assembly in continuous flow [59]	93.6 (model)	Process claims stated; recompute from SI	Solvent inventory; residence-time optimisation	Removes batch constraints; sustainability claim should be recomputed on this protocol

Provenance: *Atom economies in this table and in Table **1** derive from 33 model equations that were balanced computationally; the structure register and the balance check are provided as supporting information.*

11. CHALLENGES AND OUTLOOK

11.1. Scope Claims Outrun Validated Success Rates

A substrate table showing thirty examples is selected for what worked. Only two datasets in this review report the denominator: an 85% success rate across a 790-member GBB library [41], and pass rates of 65/251 aldehydes, 194/380 amines and 15/19 tosylmethyl isocyanides against a 50% yield threshold in a van Leusen validation [44]. They tell a more useful story than any scope figure, and the field would benefit from reporting such data routinely.

11.2. Mechanistic Evidence is Unevenly Distributed

On the criteria of Section 1.2, the classical named reactions are well characterised at Level A [21, 24-26, 30], with computational support recorded separately [29]. The scaffold-directed cascades that constitute most of the recent output are generally Level B or C, and sixteen of the twenty-four representative methods collected in Table **2** report no mechanistic test at all (Fig. **8**). Because Table **2** is restricted to methods published between 2019 and 2026, the Level A assignments for the Ugi and Biginelli manifolds rest on earlier primary studies that the table does not list. Where the terminal oxidation is left unassigned [31], neither the mass balance nor the scalability can be assessed.

11.3. Metrics are Reported Selectively

Atom economy is quoted because it is favourable and easy to calculate; reaction mass efficiency and process mass intensity, which would reveal the cost of excess reagents, solvent and chromatography, are usually absent, and calculated and measured values are seldom distinguished. The audit protocol of Section 9.3 is a minimum, not an ambition.

11.4. Catalyst Cost is Externalised

Pincer complexes and functionalised nanomaterials move the synthetic burden upstream of the reaction being celebrated, and recycling evidence rarely rises above tier R1.

11.5. Regio and Stereocontrol Remain Uneven

Asymmetric MCRs are established for the Povarov [30, 47] and Biginelli [27] manifolds but remain the exception; the combinatorial advantage of MCRs is diminished when the product is racemic.

Four directions follow (Fig. **9**). Closed-loop optimisation would attack the metric and scope problems together: high-throughput experimentation at reduced scale [68] feeds a model whose objective function combines yield with process mass intensity rather than yield alone. Continuous flow addresses the photon-flux and heat-transfer constraints that limit photochemical and high-temperature MCRs, and has already been demonstrated for a multicomponent route to fused imidazoheterocycles [59, 60]. Asymmetric catalysis, particularly through chiral phosphoric acids in cation-based manifolds, extends the platforms whose mechanisms are best understood. DNA-encoded and nanoscale library formats [44, 65] exploit exactly the properties that MCRs possess and stepwise routes do not: one-pot operation, aqueous compatibility and wide building-block availability.



Fig. (8). Mechanistic evidence reported for the 24 representative methods of Table **2**, graded on the criteria defined in Section 1.2. Two entries are Level A, five Level B and one Level C; the remaining sixteen report no mechanistic test. The well-characterised manifolds are concentrated in the classical named reactions rather than in the recent scaffold-directed cascades.

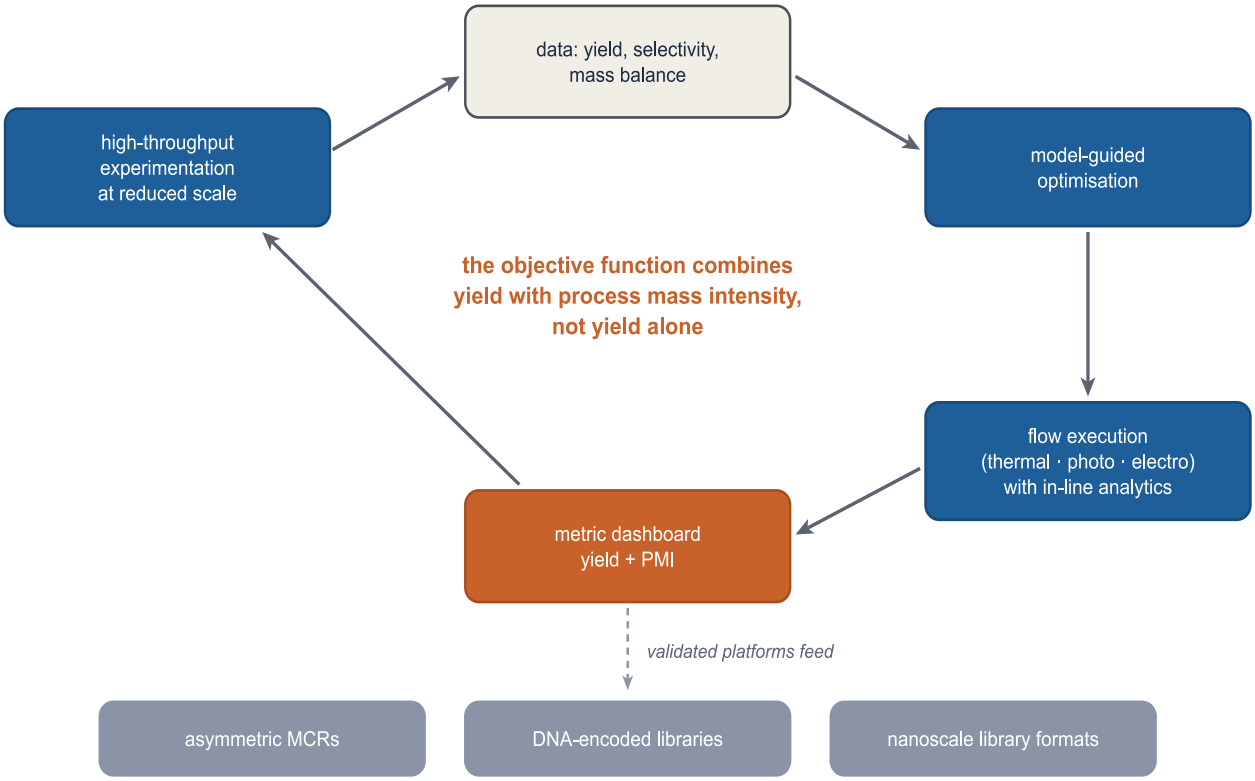


Fig. (9). A closed-loop workflow for multicomponent reaction development in which high-throughput experimentation, model-guided optimisation and flow execution are steered by an objective function that combines yield with process mass intensity. Validated platforms feed asymmetric MCRs and DNA-encoded and nanoscale library formats (Section 11).

CONCLUSION

Multicomponent reactions deserve their standing in nitrogen heterocycle synthesis, but for narrower and more specific reasons than the literature usually gives. Their advantage is isolation economy and building-block combinatorics, not atom economy, which varies little across platforms and is governed more by the nitrogen source and the terminal oxidant than by the multicomponent step. The manifolds whose intermediates have been intercepted, namely the iminium, nitrilium and N-acyliminium manifolds and the stepwise Povarov sequence, are the ones that can be optimised rationally. The recent finding that the solvent can act as a co-catalyst in a reaction as well studied as the GBB shows how much remains to be learned even there. The clearest sustainability gains come from acceptorless dehydrogenative coupling, from mechanochemistry where the comparison is measured within a single study, and from flow, in each case because the claim is tied to a quantity. The most useful change the field could make is to report the denominators: how many substrates failed, what the terminal oxidant was, and what mass of material was consumed per mass of product, with calculated and measured metrics clearly distinguished.

LIST OF ABBREVIATIONS

AE	=	Atom Economy
CuAAC	=	Copper-Catalysed Azide–Alkyne Cycloaddition
DDQ	=	2,3-dichloro-5,6-dicyano-1,4-benzoquinone
GBB	=	Groebke–Blackburn–Bienaymé
MCRs	=	Multicomponent Reactions
PMI	=	Process Mass Intensity
RME	=	Reaction Mass Efficiency

AUTHORS' CONTRIBUTIONS

A.U. contributed to the study conception and design, data collection, data analysis and interpretation, and manuscript writing. S.C.Y.S. contributed to the study conception and design, data analysis and interpretation, manuscript writing, supervision, and critical revision of the manuscript.

ETHICAL APPROVAL & INFORMED CONSENT

Ethical approval and informed consent were not required for this study, as it is a review of published literature and did not involve human participants, human-derived data, or animals.

AVAILABILITY OF DATA AND MATERIAL

No new data were generated in this study.

FUNDING

None.

CONFLICT OF INTEREST

The authors declare that they have no competing interests that could have influenced the conduct or findings of this study.

ACKNOWLEDGEMENTS

Declared none.

DECLARATION OF AI

The authors used ChatGPT solely for language editing during the preparation of this manuscript. All AI-assisted content was reviewed, verified, and approved by the authors, who take full responsibility for the final content of the manuscript.

REFERENCES

[1] E. Vitaku, D. T. Smith, J. T. Njardarson, Analysis of the Structural Diversity, Substitution Patterns, and Frequency of Nitrogen Heterocycles among U.S. FDA Approved Pharmaceuticals. *J. Med. Chem.* **2014**, *57* (24), 10257–10274. https://doi.org/10.1021/jm501100b

[2] C. M. Marshall, J. G. Federice, C. N. Bell, P. B. Cox, J. T. Njardarson, An Update on the Nitrogen Heterocycle Compositions and Properties of U.S. FDA-Approved Pharmaceuticals (2013–2023)., *J. Med. Chem.* **2024**, *67* (14), 11622–11655. https://doi.org/10.1021/acs.jmedchem.4c01122

[3] A. Dömling, W. Wang, K. Wang, Chemistry and Biology of Multicomponent Reactions. *Chem. Rev.* **2012**, *112* (6), 3083–3135. https://doi.org/10.1021/cr100233r

[4] R. C. Cioc, E. Ruijter, R. V. A. Orru, Multicomponent reactions: advanced tools for sustainable organic synthesis. *Green Chem.* **2014**, *16* (6), 2958–2975. https://doi.org/10.1039/C4GC00013G

[5] G. Graziano, A. Stefanachi, M. Contino, R. Prieto-Díaz, A. Ligresti, P. Kumar, A. Scilimati, E. Sotelo, F. Leonetti, Multicomponent Reaction-Assisted Drug Discovery: A Time- and Cost-Effective Green Approach Speeding Up Identification and Optimization of Anticancer Drugs. *Int. J. Mol. Sci.* **2023**, *24* (7), 6581. https://doi.org/10.3390/ijms24076581

[6] P. Nadal Rodríguez, O. Ghashghaei, A. Bagán, C. Escolano, R. Lavilla, Heterocycle-Based Multicomponent Reactions in Drug Discovery: From Hit Finding to Rational Design. *Biomedicines* **2022**, *10* (7), 1488. https://doi.org/10.3390/biomedicines10071488

[7] Mallappa, M. Chahar, N. Choudhary, K. K. Yadav, M. T. Qasim, R. Zairov, A. Patel, V. K. Yadav, M. Jangir, Recent advances in the synthesis of nitrogen-containing heterocyclic compounds *via* multicomponent reaction and their emerging biological applications: a review. *J. Iran. Chem. Soc.* **2025**, *22*, 1–33. https://doi.org/10.1007/s13738-024-03142-3

[8] A. Boltjes, A. Dömling, The Groebke–Blackburn–Bienaymé Reaction. *Eur. J. Org. Chem.* **2019**, *2019* (42), 7007–7049. https://doi.org/10.1002/ejoc.201901124

[9] C. Martini, M. I. D. Mardjan, A. Basso, The Groebke–Blackburn–Bienaymé reaction in its maturity: innovation and improvements since its 21st birthday (2019–2023). *Beilstein J. Org. Chem.* **2024**, *20*, 1839–1879. https://doi.org/10.3762/bjoc.20.162

[10] C. M. Winkelhake, M. Q. Hartley, P. Yadav, H. O. Sintim. Revisiting multicomponent Doebner and Povarov quinoline synthesis for modern-day drug-discovery. *Org. Biomol. Chem.* **2026**, *24* (35), 7209–7255. https://doi.org/10.1039/d6ob00871b

[11] G. A. Coppola, S. Pillitteri, E. V. Van der Eycken, S.-L. You, U. K. Sharma. Multicomponent reactions and photo/electrochemistry join forces: atom economy meets energy efficiency. *Chem. Soc. Rev.* **2022**, *51* (6), 2313–2382. https://doi.org/10.1039/D1CS00510C

[12] Y. Chen, B. Huang. Harnessing the synergistic power of light and electricity: an emerging frontier in catalytic heterocycle synthesis. *Org. Chem. Front.* **2025**, *12* (23), 6614–6630. https://doi.org/10.1039/d5qo01097g

[13] H. G. O. Alvim, E. N. da Silva Júnior, B. A. D. Neto. What do we know about multicomponent reactions? Mechanisms and trends for the Biginelli, Hantzsch, Mannich, Passerini and Ugi MCRs. *RSC Adv.* **2014**, *4* (97), 54282–54299. https://doi.org/10.1039/C4RA10651B

[14] M. O. Rodrigues, M. N. Eberlin. B. A. D. Neto, How and Why to Investigate Multicomponent Reactions Mechanisms? A Critical Review. *Chem. Rec.* **2021**, *21* (10), 2762–2781. https://doi.org/10.1002/tcr.202000165

[15] B. A. D. Neto, M. N. Eberlin. J. Sherwood, Solvent Screening Is Not Solvent Effect: A Review on the Most Neglected Aspect of Multicomponent Reactions. *Eur. J. Org. Chem.* **2022**, *2022* (30), e202200172. https://doi.org/10.1002/ejoc.202200172

[16] R. A. Sheldon. Metrics of Green Chemistry and Sustainability: Past, Present, and Future. *ACS Sustainable Chem. Eng.* **2018**, *6* (1), 32–48. https://doi.org/10.1021/acssuschemeng.7b03505

[17] C. Jiménez-González, C. S. Ponder, Q. B. Broxterman, J. B. Manley. Using the Right Green Yardstick: Why Process Mass Intensity Is Used in the Pharmaceutical Industry To Drive More Sustainable Processes. *Org. Process Res. Dev.* **2011**, *15* (4), 912–917. https://doi.org/10.1021/op200097d

[18] L. F. Tietze. Domino Reactions in Organic Synthesis. *Chem. Rev.* **1996**, *96* (1), 115–136. https://doi.org/10.1021/cr950027e

[19] A. Dömling, I. Ugi. Multicomponent Reactions with Isocyanides. *Angew. Chem. Int. Ed.* **2000**, *39* (18), 3168–3210. https://doi.org/10.1002/1521-3773(20000915)39:18%3C3168::AID-ANIE3168%3E3.0.CO;2-U

[20] H. Bienaymé, K. Bouzid,.A New Heterocyclic Multicomponent Reaction For the Combinatorial Synthesis of Fused 3-Aminoimidazoles. *Angew. Chem. Int. Ed.* **1998**, *37* (16), 2234–2237. https://doi.org/10.1002/(SICI)1521-3773(19980904)37:16%3C2234::AID-ANIE2234%3E3.0.CO;2-R

[21] G. A. Medeiros, W. A. da Silva, G. A. Bataglion. D. A. C. Ferreira, H. C. B. de Oliveira, M. N. Eberlin, B. A. D. Neto, Probing the mechanism of the Ugi four-component reaction with charge-tagged reagents by ESI-MS(/MS). *Chem. Commun.* **2014**, *50* (3), 338–340. https://doi.org/10.1039/c3cc47156j

[22] N. Chéron, R. Ramozzi, L. El Kaïm, L. Grimaud. P. Fleurat-Lessard. Challenging 50 Years of Established Views on Ugi Reaction: A Theoretical Approach. *J. Org. Chem.* **2012**, *77* (3), 1361–1366. https://doi.org/10.1021/jo2021554

[23] M. H. R. Carvalho, J. P. R. S. Ribeiro, P. P. De Castro, S. T. A. Passos, B. A. D. Neto, H. F. Dos Santos, G. W. Amarante. Solvent Dependent Competitive Mechanisms for the Ugi Multicomponent Reaction: A Joint Theoretical and Experimental Study in the α-Acyl Aminocarboxamides vs α-Amino Amidines Formation. *J. Org. Chem.* **2022**, *87* (16), 11007–11020. https://doi.org/10.1021/acs.joc.2c01272

[24] M. H. R. Carvalho, P. P. De Castro, P. Beck, H. F. Dos Santos, F. Machado, J. R. Correa, B. A. D. Neto, G. W. Amarante, Solvents' and Reagents' Noninnocent Roles in the Groebke–Blackburn–Bienaymé (GBB) Multicomponent Reaction: Experimental and Computational Evidence, *ACS Org. Inorg. Au* **2025**, *5* (4), 288–298. https://doi.org/10.1021/acsorginorgau.5c00049

[25] C. O. Kappe. A Reexamination of the Mechanism of the Biginelli Dihydropyrimidine Synthesis. Support for an N-Acyliminium Ion Intermediate. *J. Org. Chem.* **1997**, *62* (21), 7201–7204. https://doi.org/10.1021/jo971010u

[26] R. O. M. A. De Souza, E. T. da Penha, H. M. S. Milagre, S. J. Garden, P. M. Esteves, M. N. Eberlin, O. A. C. Antunes. The Three-Component Biginelli Reaction: A Combined Experimental and Theoretical Mechanistic Investigation. *Chem. Eur. J.* **2009**, *15* (38), 9799–9804. https://doi.org/10.1002/chem.200900470

[27] H. G. O. Alvim, D. L. J. Pinheiro, V. H. Carvalho-Silva, M. Fioramonte, F. C. Gozzo, W. A. da Silva, G. W. Amarante, B. A. D. Neto. Combined Role of the Asymmetric Counteranion-Directed Catalysis (ACDC) and Ionic Liquid Effect for the Enantioselective Biginelli Multicomponent Reaction. *J. Org. Chem.* **2018**, *83* (19), 12143–12153. https://doi.org/10.1021/acs.joc.8b02101

[28] H. G. O. Alvim, T. B. Lima, A. L. de Oliveira, H. C. B. de Oliveira, F. M. Silva, F. C. Gozzo, R. Y. Souza, W. A. da Silva, B. A. D. Neto. Facts, Presumptions, and Myths on the Solvent-Free and Catalyst-Free Biginelli Reaction. What is Catalysis for?. *J. Org. Chem.* **2014**, *79* (8), 3383–3397. https://doi.org/10.1021/jo5001498

[29] Y. A. Rodríguez-Núñez, J. Sánchez-Márquez, J. Quintero-Saumeth, C. J. Guerra, E. Polo-Cuadrado, D. Villaman, C. A. Fica-Cornejo, A. R. R. Bohórquez. Mechanistic insights on the Lewis acid-catalyzed three-component cationic Povarov reaction: synthesis of N-propargyl 1,2,3,4-tetrahydroquinolines. *RSC Adv.* **2025**, *15* (15), 11799–11810. https://doi.org/10.1039/d5ra01375e

[30] P. Kisszékelyi, T. Doblejová, E. Rakovský, R. Šebesta. Mechanochemical Stereoselective Povarov Reaction *via* Brønsted Acid Organocatalysis. *Chem. Eur. J.* **2025**, *31* (69), e02466. https://doi.org/10.1002/chem.202502466

[31] S. Rashidi, M. Soleiman-Beigi. Natural asphalt oxide-grafted carboxylic acid: a sustainable heterogeneous catalyst for synthesis of pyrano[2,3-c]pyrazoles and 2-amino-3-cyanopyridines in water. *RSC Adv.* **2025**, *15* (31), 25274–25290. https://doi.org/10.1039/d5ra03786g

[32] Y. Zhang, X. Ma, X. Zhou, K. Jiang, L. Gu, X. Li, Y. Zhu, B. Peng. Green Synthesis of 1,4-Dihydropyridines through Catalyst-Free Multicomponent Hantzsch Reaction in an Undergraduate Teaching Laboratory. *J. Chem. Educ.* **2025**, *102* (3), 1215–1222. https://doi.org/10.1021/acs.jchemed.4c01069

[33] S. Momeni, R. Ghorbani-Vaghei. Synthesis, properties, and application of the new nanocatalyst of double layer hydroxides in the one-pot multicomponent synthesis of 2-amino-3-cyanopyridine derivatives. *Sci. Rep.* **2023**, *13*, 1627. https://doi.org/10.1038/s41598-023-27940-6

[34] K. Ikeno, H. Oku, K. Rakumitsu, M. Kitajima, H. Ishikawa. Modified Bohlmann–Rahtz Pyridine Synthesis for Cyclic Ketones. *Chem. Eur. J.* **2025**, *31* (22), e202500298. https://doi.org/10.1002/chem.202500298

[35] K. Perumal, M. Shanthi, V. Hemamalini, B. Shankar, S. Ramesh. Metal-free, iodine-mediated multicomponent synthesis of bis-pyrazolo-pyridine derivatives. *Chem. Commun.* **2026**, *62* (23), 6356–6359. https://doi.org/10.1039/d6cc00245e

[36] N. Deibl, K. Ament, R. Kempe. A Sustainable Multicomponent Pyrimidine Synthesis. *J. Am. Chem. Soc.* **2015**, *137* (40), 12804–12807. https://doi.org/10.1021/jacs.5b09510

[37] N. Deibl, R. Kempe. Manganese-Catalyzed Multicomponent Synthesis of Pyrimidines from Alcohols and Amidines. *Angew. Chem. Int. Ed.* **2017**, *56* (6), 1663–1666. https://doi.org/10.1002/anie.201611318

[38] C. Savarimuthu Selvan, R. Rengan, J. G. Malecki. One-Pot Sustainable Synthesis of Highly Substituted Pyrimidines *via* Acceptorless Dehydrogenative Annulation of Alcohols Using Pincer Ni(II)–NNS Catalysts. *J. Org. Chem.* **2024**, *89* (16), 11148–11160. https://doi.org/10.1021/acs.joc.4c00587

[39] P. Kukreti, Y. Hitomi, K. Ghosh. A Strategic Advance from Pincer Complexes to Hexadentate-Co(III) Catalyst for Metal–Ligand Cooperative Activation of Primary Alcohols to Access Highly Functionalized Pyrimidines. *Chem. Eur. J.* **2025**, *31* (56), e02258. https://doi.org/10.1002/chem.202502258

[40] P. K. Sekar, A. Pennamuthiriyan, R. Rengan. Sustainable Synthesis of Pyrimidines by [NNO]-Pincer-Supported Nickel(II) Complexes *via* Dehydrogenative Annulation of Alcohols. *J. Org. Chem.* **2025**, *90* (28), 9845–9858. https://doi.org/10.1021/acs.joc.5c00821

[41] E. V. Govor, V. Naumchyk, I. Nestorak, D. S. Radchenko, D. Dudenko, Y. S. Moroz, O. D. Kachkovsky, O. O. Grygorenko. Generation of multimillion chemical space based on the parallel Groebke–Blackburn–Bienaymé reaction. *Beilstein J. Org. Chem.* **2024**, *20*, 1604–1613. https://doi.org/10.3762/bjoc.20.143

[42] H. Okai, K. Tanimoto, R. Ohkado, H. Iida. Multicomponent Synthesis of Imidazo[1,2-a]pyridines: Aerobic Oxidative Formation of C–N and C–S Bonds by Flavin–Iodine-Coupled Organocatalysis. *Org. Lett.* **2020**, *22* (20), 8002–8006. https://doi.org/10.1021/acs.orglett.0c02929

[43] L. Guo, Y. Ding, H. Wang, Y. Liu, Q. Qiang, Q. Luo, F. Song, C. Li. Imidazo[1,2-a]pyridine derivatives synthesis from lignin β-O-4 segments *via* a one-pot multicomponent reaction. *iScience* **2023**, *26* (6), 106834. https://doi.org/10.1016/j.isci.2023.106834

[44] Y. Xie, M. Huang, Y. Jiang, X. Miao, H. Wang, Q. Zhang, D. Dai, X. Zeng, Q. Yang, W. Su, A. L. Satz, L. Kuai. Van Leusen Imidazole Synthesis for One-Bead-One-Compound DNA-Encoded Libraries. *Bioconjugate Chem.* **2025**, *36* (9), 2013–2019. https://doi.org/10.1021/acs.bioconjchem.5c00317

[45] M. Amiri, N. Bagherzadeh, A. R. Sardarian. Novel, nanomagnetic and recoverable copper(0)-catalyst in one-pot access to 1,4-disubstituted 1,2,3-triazoles and 5-substituted 1H-tetrazoles in water. *R. Soc. Open Sci.* **2025**, *12* (2), 241322. https://doi.org/10.1098/rsos.241322

[46] D. Xing, Q. Zhao, L. Fu. Povarov-type Reaction of Anilines, Aqueous Acetaldehyde, and tBuONO for Access to N-Nitroso-1,2,3,4-tetrahydroquinolines. *Org. Lett.* **2026**, *28* (17), 5609–5613. https://doi.org/10.1021/acs.orglett.6c01331

[47] A. Brion, V. Martini, M. Lombard, P. Retailleau, N. Della Ca', L. Neuville, G. Masson. Phenolic Dienes as Highly Selective Dienophiles in the Asymmetric Organocatalyzed Three-Component Vinylogous Povarov Reaction. *J. Org. Chem.* **2024**, *89* (17), 12298–12306. https://doi.org/10.1021/acs.joc.4c01239

[48] X. Zhang, M. Liu, D. Zhan, M. Kaur, J. P. Jasinski, W. Zhang. Three-component [3 + 2] cycloaddition for regio- and diastereoselective synthesis of spirooxindole-pyrrolidines. *New J. Chem.* **2022**, *46* (8), 3866–3870. https://doi.org/10.1039/d1nj05538k

[49] R. S. Kumar, D. M. Al-Thamili, A. I. Almansour, N. Arumugam, N. Dege. [Bmim]Br Accelerated One-Pot Three-Component Cascade Protocol for the Construction of Spirooxindole–Pyrrolidine Heterocyclic Hybrids. *Molecules* **2020**, *25* (20), 4779. https://doi.org/10.3390/molecules25204779

[50] M. Palomba, E. De Monte, A. Mambrini, L. Bagnoli, C. Santi, F. Marini. A three-component [3 + 2]-cycloaddition/elimination cascade for the synthesis of spirooxindole-pyrrolizines. *Org. Biomol. Chem.* **2021**, *19* (3), 667–676. https://doi.org/10.1039/d0ob02321c

[51] J. H. Clark, D. J. Macquarrie, J. Sherwood, The Combined Role of Catalysis and Solvent Effects on the Biginelli Reaction: Improving Efficiency and Sustainability, *Chem. Eur. J.* **2013**, *19* (16), 5174–5182. https://doi.org/10.1002/chem.201204396

[52] P. Kukreti, P. Datta, R. Chauhan, T. Pattnaik, K. Sharma, K. Ghosh. Phosphine-Free NNN Pincer Supported Cu(II) Catalysts for Sustainable Multi-Component Synthesis of Pyrazolines and Pyrimidines *via* Dehydrogenation of Renewable Primary Alcohols. *Chem. Asian J.* **2025**, *20* (22), e70278. https://doi.org/10.1002/asia.70278

[53] M. Rueping, C. Vila. Visible Light Photoredox-Catalyzed Multicomponent Reactions. *Org. Lett.* **2013**, *15* (9), 2092–2095. https://doi.org/10.1021/ol400317v

[54] Y. Li, Y. Zhang, J. Wang, D. Xia, M. Zhuo, L. Zhu, D. Li, S.-F. Ni, Y. Zhu, W.-D. Zhang. Visible-Light-Mediated Three-Component Strategy for the Synthesis of Isoxazolines and Isoxazoles. *Org. Lett.* **2024**, *26* (15), 3130–3134. https://doi.org/10.1021/acs.orglett.4c00671

[55] J. K. Pathak, N. Rastogi. One-pot three-component synthesis of hydroxyacetylated imidazo[1,2-a]pyridines *via* visible-light-mediated halogen atom transfer. *Org. Biomol. Chem.* **2026**, *24* (9), 1883–1888. https://doi.org/10.1039/d6ob00033a

[56] S.-Y. Ren, Q. Zhou, H.-Y. Zhou, L.-W. Wang, O. M. Mulina, S. A. Paveliev, H.-T. Tang, A. O. Terent'ev, Y.-M. Pan, X.-J. Meng. Three-Component Electrochemical Aminoselenation of 1,3-Dienes. *J. Org. Chem.* **2023**, *88* (9), 5760–5771. https://doi.org/10.1021/acs.joc.3c00214

[57] D. Prat, A. Wells, J. Hayler, H. Sneddon, C. R. McElroy, S. Abou-Shehada, P. J. Dunn. CHEM21 selection guide of classical- and less classical-solvents. *Green Chem.* **2016**, *18* (1), 288–296. https://doi.org/10.1039/C5GC01008J

[58] N. Fantozzi, J.-N. Volle, A. Porcheddu, D. Virieux, F. García, E. Colacino. Green metrics in mechanochemistry. *Chem. Soc. Rev.* **2023**, *52* (19), 6680–6714. https://doi.org/10.1039/d2cs00997h

[59] B. J. M. Baker, W. J. Kerr, D. M. Lindsay, V. K. Patel, D. L. Poole. A sustainable and scalable multicomponent continuous flow process to access fused imidazoheterocycle pharmacophores. *Green Chem.* **2021**, *23* (1), 280–287. https://doi.org/10.1039/D0GC03675G

[60] M. H. R. Carvalho, P. P. de Castro, K. T. de Oliveira, G. W. Amarante. Enhancing Efficiency and Sustainability: Unleashing the Potential of Continuous Flow in Multicomponent Reactions. *ChemSusChem* **2025**, *18* (4), e202401840. https://doi.org/10.1002/cssc.202401840

[61] T. U. Mayer, T. M. Kapoor, S. J. Haggarty, R. W. King, S. L. Schreiber, T. J. Mitchison. Small Molecule Inhibitor of Mitotic Spindle Bipolarity Identified in a Phenotype-Based Screen. *Science* **1999**, *286* (5441), 971–974. https://doi.org/10.1126/science.286.5441.971

[62] M. Konstantinidou, F. Magari, F. Sutanto, J. Haupenthal, V. R. Jumde, M. Y. Ünver, A. Heine, C. J. Camacho, A. K. H. Hirsch, G. Klebe, A. Dömling. Rapid Discovery of Aspartyl Protease Inhibitors Using an Anchoring Approach. *ChemMedChem* **2020**, *15* (8), 680–684. https://doi.org/10.1002/cmdc.202000024

[63] R. Butera, M. Ważyńska, K. Magiera-Mularz, J. Plewka, B. Musielak, E. Surmiak, D. Sala, R. Kitel, M. de Bruyn, H. W. Nijman, P. H. Elsinga, T. A. Holak. A. Dömling, Design, Synthesis, and Biological Evaluation of Imidazopyridines as PD-1/PD-L1 Antagonists. *ACS Med. Chem. Lett.* **2021**, *12* (5), 768–773. https://doi.org/10.1021/acsmedchemlett.1c00033

[64] K. B. Owusu, J. Samal, D. E. Hernandez, H. O. Sintim. Orally bioavailable STING antagonist synthesized *via* multi-component Povarov–Doebner type reaction. *Chem. Commun.* **2024**, *60* (83), 11932–11935. https://doi.org/10.1039/d4cc03228d

[65] Y. An, J. Lee, H. Seo, S. Bae, J. Kang, J. Lee, J. Kim, M. H. Nam, M. Song, G. T. Hwang. Groebke–Blackburn–Bienaymé Reaction for DNA-Encoded Library Technology. *Org. Lett.* **2023**, *25* (24), 4445–4450. https://doi.org/10.1021/acs.orglett.3c01366

[66] Maji, M.; Kundu, S. Cooperative ruthenium complex catalyzed multicomponent synthesis of pyrimidines. *Dalton Trans.* **2019**, *48* (47), 17479–17487. https://doi.org/10.1039/c9dt04040d

[67] Mondal, R.; Chakraborty, G.; Guin, A. K.; Sarkar, S.; Paul, N. D. Iron-Catalyzed Alkyne-Based Multicomponent Synthesis of Pyrimidines under Air. *J. Org. Chem.* **2021**, *86* (19), 13186–13197. https://doi.org/10.1021/acs.joc.1c00867

[68] K. Gao, S. Shaabani, R. Xu, T. Zarganes-Tzitzikas, L. Gao, M. Ahmadianmoghaddam, M. R. Groves, A. Dömling. Nanoscale, automated, high throughput synthesis and screening for the accelerated discovery of protein modifiers. *RSC Med. Chem.* **2021**, *12* (5), 809–818. https://doi.org/10.1039/D1MD00087J